then there should be higher terms of z in the function $\gamma_1(z)$. Now from eq A7 through A9, it follows that at large scattering angles

$$\lim_{h_3 \to \infty} I_s(h_3) = I_e(\rho_1 - \rho_2)^2 S_p^2 h_3^{-2} \quad \text{(A10)}$$

For the two-phase system composed of N perfectly oriented lamellae, S_p in eq A10 should be replaced with S given by

$$S = NS_p \quad \text{(A11)}$$

where S is the total surface area of the lamellar microphase system normal to the z axis. Therefore, the scattered intensity at large angle tail for the completely oriented ideal two-phase structure is given by

$$\lim_{h_3 \to \infty} I_s(h_3) = I_e(\rho_1 - \rho_2)^2 S^2 h_3^{-2} \quad \text{(A12)}$$

Equation A12 corresponds to eq A5 for the isotropic and ideal two-phase structure. The reduced scattering angle h_3 in eq A12 also corresponds to the variable $2\pi s$ in the text, so that eq A12 can be rewritten by

$$\lim_{s \to \infty} I_s = [I_e(\rho_1 - \rho_2)^2 S^2 / 4\pi^2] s^{-2} \quad \text{(A13)}$$

References and Notes

(1) Presented partly at the 24th Symposium on Polymer Chemistry, Japan, Osaka University, Nov. 6, 1975.
(2)(a) T. Hashimoto, K. Nagatoshi, A. Todo, H. Hasegawa, and H. Kawai, *Macromolecules*, **7**, 364 (1974); (b) D. J. Blundell, *Acta Crystallogr., Ser. A*, **26**, 472, 476 (1970).
(3) D. J. Meier, *J. Polym. Sci., Part C.*, **26**, 81 (1969).
(4) D. J. Meier, *Polym. Prepr., Am. Chem. Soc., Div. Polym. Chem.*, **11**, 400 (1970).
(5) D. J. Meier, *Polym. Prepr., Am. Chem. Soc., Div. Polym. Chem.*, **15**, 171 (1974).
(6) T. Inoue and D. J. Meier, paper presented at the 24th Symposium on Polymer Chemistry, Japan, Osaka University, Nov. 6, 1975.
(7) E. Helfand, *Polym. Prepr., Am. Chem. Soc., Div. Polym. Chem.*, **14**, 970 (1973).
(8) E. Helfand, "Recent Advance in Blends, Grafts, and Blocks", L. H. Sperling, Ed., Plenum Press, New York, N.Y., 1974.
(9) E. Helfand, *Macromolecules*, **8**, 552 (1975).
(10) E. Helfand and Y. Tagami, *J. Chem. Phys.*, **56**, 3592 (1972).
(11) T. Inoue, T. Soen, T. Hashimoto, and H. Kawai, *J. Polym. Sci., Part A-2*, **17**, 1283 (1969).
(12) E. Helfand, *J. Chem. Phys.*, **62**, 999 (1975).
(13) See, for example, A. Guinier and G. Fournet, "Small-angle Scattering of X-rays", Wiley, New York, N.Y., 1955.
(14) G. Porod, *Kolloid Z. Z. Polym.*, **124(2)**, 83 (1951); **125(1)**, 51 (1952); **125(2)**, 108 (1952).
(15) P. Debye, H. R. Anderson, Jr., and H. Brumberger, *J. Appl. Phys.*, **28**, 679 (1957).
(16) C. G. Vonk, *J. Appl. Crystallogr.*, **6**, 81 (1973).
(17) D. F. Leary and M. C. Williams, *J. Polym. Sci., Part B*, **8**, 335 (1970); *J. Polym. Sci., Polym. Phys, Ed.*, **11**, 345 (1973).
(18) E. Helfand and A. M. Sapse, *J. Chem. Phys.*, **62**, 1327 (1975).
(19) E. Helfand, *Acc. Chem. Res.*, **8**, 295 (1975).
(20) E. Helfand and Z. R. Wasserman, to be published in *Macromolecules*.
(21) D. J. Meier, private communication.
(22) E. Helfand, private communication.
(23) A. Todo, M. Fujimura, T. Hashimoto, and H. Kawai, to be published.
(24) The effect of truncating the higher order terms has been recently examined by Hashimoto et al.[23] The results indicate that inclusion of higher order terms yields greater values for σ and t.
(25) It is noted that the first maximum of amorphous scattering of polystyrene is located at the Bragg angle (2θ) 9.8°, while the maximum of polyisoprene is at ca. 14°.
(26) It should be noted that the restriction of the symmetric block has been removed in the recent calculations of Meier.[21]
(27) It is pointed out by Helfand[22] that the Debye length t_D should be divided by a factor of $3^{1/2}$ when it is compared with the interphase thickness. This is because the interphase width is in one direction only, while the Debye length refers to an isotropic phenomenon.

Magic-Angle ^{13}C NMR Analysis of Motion in Solid Glassy Polymers

Jacob Schaefer,* E. O. Stejskal, and R. Buchdahl

Monsanto Company, Corporate Research Department, St. Louis, Missouri 63166.

Received June 14, 1976

ABSTRACT: The dipolar-decoupled, natural abundance Fourier transform and cross-polarization ^{13}C NMR spectra of seven glassy polymers have been obtained at 22.6 MHz, both with and without 3-kHz mechanical spinning at the magic angle. The 100-Hz resolution achieved by the spinning produces spectra of the solids almost as detailed as the standard spectra of the same polymers in solution. This kind of resolution allows individual lines to be assigned to chemically unique carbons both in the side and main chains of the polymers. Spin–lattice, nuclear-Overhauser, rotating-frame, and cross-polarization relaxation parameters have been measured for individual carbon lines at room temperature. The ^{13}C rotating frame relaxation times ($T_{1\rho}$) at 32 kHz can be shown to be dominated by spin–lattice processes rather than spin–spin processes. This means that the $T_{1\rho}$'s contain information about the motions of the polymers in the 10–50 kHz region, while the cross-polarization relaxation times (T_{CH}) contain information about the near static interactions. The spin–lattice and nuclear-Overhauser relaxation parameters contain information about the motions in the 5–30-MHz regions. Interpretation of the $T_{1\rho}$'s of these polymers emphasizes the dynamic heterogeneity of the glassy state. Details of the relaxation processes establish the short-range nature of certain low-frequency side-group motions, while clearly defining the long-range cooperative nature of some of the main-chain motions, the latter not consistent with a local-mode interpretation of motion. These motions involve cooperative torsional oscillations within conformations rather than jumps from one conformation to another. The ratio of T_{CH} to $T_{1\rho}$ for protonated carbons in the main chain of each polymer is found to have a direct correlation with the toughness or impact strength for all seven polymers. This empirical correlation is rationalized in terms of energy dissipation for chains in the amorphous state in which low-frequency cooperative motions (and ultimately flow) are determined by the same inter- and intra-chain steric interactions which influence the NMR relaxation parameters.

I. Introduction

We have three objectives in this paper. First, we will show that the rotating-frame ^{13}C relaxation parameters obtained from high-resolution ^{13}C NMR spectra of glassy polymers can be interpreted unambiguously in terms of the side- and main-chain motions of the polymers in the solid state (sections IV–VI). Second, we will show that an understanding of the

details of the motion can lead to some clarifications of the dynamic nature of the glassy state in noncrystalline polymers (section V). And, finally, we will show how the ^{13}C relaxation parameters describing the motions of the polymers can be related to macroscopic properties of the glassy state such as the mechanical impact strength (section VII).

High-resolution, natural abundance, ^{13}C NMR spectra of solid polymers have been reported before.[1] In these experiments two kinds of line narrowing techniques are employed. Dipolar broadening of the ^{13}C lines by protons is removed by strong resonant decoupling (referred to as dipolar decoupling) using ^{1}H decoupling radiofrequency (rf) fields of about 10 G. These decoupling fields are comparable to the proton line widths. In most cases the resulting ^{13}C NMR spectra are still severely complicated by overlapping chemical shift anisotropies, so that, in general, only a few broad lines are observed. A dramatic improvement in the resolution of such spectra can be achieved by fashioning rotors[2] from the solid polymers and obtaining dipolar-decoupled spectra while mechanically spinning these rotors at the so-called "magic angle", at frequencies somewhat greater than the dispersion of chemical shifts.[1]

Even with the resolution achieved by a combination of dipolar decoupling and magic-angle spinning, a Fourier transform (FT) experiment on a solid polymer still has a serious limitation. Namely, a delay time of several ^{13}C spin–lattice relaxation times (T_1) must be tolerated before data sampling can be repeated. These repetitions are necessary to provide a suitably strong signal by a time-averaging process. Since some ^{13}C T_1's for solid polymers are on the order of tens of seconds,[1] the time-averaging process becomes tedious. These delays can be avoided, however, by performing a matched spin-lock (or Hartmann–Hahn) cross-polarization (CP) experiment.[3,4] With this technique, polarization of the carbons is achieved by a transfer from nearby protons, spin-locked in their own rf field, via static dipolar interactions in a time T_{CH}(SL).[5] This transfer is a spin–spin or T_2-type process and generally requires no more than 100 μs.[1] Most importantly, the CP transfer can be repeated and more data accumulated after allowing the *protons* to repolarize in the static field.[6] For glassy polymers near room temperature, this is more efficient than ^{13}C repolarization by spin–lattice processes and generally occurs in less than a half second.[7]

We have discovered that cross polarization and magic-angle spinning are compatible. That is, despite reasonable fears to the contrary,[1,4] for a wide variety of polymer systems near room temperature, efficient ^{1}H–^{13}C CP transfers do, in fact, occur under magic-angle spinning conditions. Thus, the 3-kHz magic-angle spinning does not totally eliminate, by motional averaging, the dipolar interactions required for transfer of magnetization from polarized nonbonded protons to nearby quaternary carbons. Strong signals are obtained from all types of carbons, quaternary, methine, methylene, and methyl, under 3-kHz magic-angle spinning conditions. The presence of strong signals from all carbons naturally greatly simplifies the interpretation of the CP ^{13}C NMR spectra of solid polymers.

With individual lines resolved for individual carbons, a variety of relaxation experiments can be performed and interpreted in terms of the motions of the polymers in the solid state. However, spin–lattice and nuclear-Overhauser relaxation measurements[1] not only are subject to sensitivity problems associated with the long time delays mentioned earlier, they also lead to ^{13}C relaxation parameters which are most sensitive to motions of the polymer in the 20-MHz range.[8] While such information is useful and interesting,[1] it is not likely to result in an understanding of the structure and dynamics of glassy polymers. What is needed is a high-sensitivity experiment leading to ^{13}C relaxation parameters which contain information about motions of the polymer near 20 kHz, a frequency range likely to be directly related to important, but relatively slow, main-chain motions of polymers well below their glass transition temperatures.[9]

It is well known that an ^{1}H rotating-frame relaxation time ($T_{1\rho}$) is sensitive to motions associated with frequencies in the 10–100 kHz range.[10] By a NMR spin-locking process, the lifetime of the ^{1}H magnetization in an effective applied rf field of 10–20 G (rather than the usual 10–20 kG of the static magnetic field) can be measured and, for glassy polymers near room temperature, associated with motional effects.[11] Of course, the usual problem with *proton* relaxation times in solid polymers is present. The observed ^{1}H $T_{1\rho}$ is an *average* over all the protons in the sample as a result of spin diffusion.[11] Thus, a simple, direct interpretation of ^{1}H relaxation data in terms of the various types of motions of the polymer is not possible.

The corresponding ^{13}C $T_{1\rho}$ experiment is not confused by spin diffusion between carbons because their low natural abundance ensures a physical separation within the solid and hence a slow spin diffusion or transfer rate. Furthermore, we have discovered, from adiabatic demagnetization measurements, that for polymers near room temperature, the transfer of polarization from carbons locked in their rotating field to nearby *un*polarized protons is also a relatively slow process. Thus, the observed relatively short ^{13}C $T_{1\rho}$'s are dominated by rotating-frame *spin–lattice* processes. That is, the $T_{1\rho}$'s are determined by spectral density at the rotating-frame Larmor frequency arising from the effect of molecular *motion* within the lattice on internuclear dipolar interactions.

We have measured, at room temperature, the ^{13}C $T_{1\rho}$ and T_{CH}(SL) for seven noncrystalline glassy polymers under magic-angle spinning conditions. The former relaxation parameter is sensitive to motions near 30 kHz and the latter to near static interactions. Both experiments use efficient CP techniques to obtain a net carbon magnetization. All the polymers investigated are examples of high molecular weight, commercial plastics and span a wide range of mechanical behavior. The polymers include poly(methyl methacrylate), polycarbonate, poly(phenylene oxide), polystyrene, polysulfone, poly(ether sulfone), and poly(vinyl chloride). The magic-angle CP ^{13}C NMR spectra of these polymers are well enough resolved to permit an unambiguous identification of resonances arising from side-chain carbons as well as those arising from main-chain carbons, and hence an analysis of the relaxation parameters in terms of the various kinds of motions of the polymer in the solid state. In the following sections, we will use the new information available from the magic-angle CP ^{13}C NMR experiment to answer some questions fundamental to an understanding of glassy polymers.

II. Details of the Experiments

(A) Spin Lock and Adiabatic Demagnetization Rotating Frame Procedures. Carbon-13 NMR spectra were obtained at room temperature using a modified Bruker HFX-90 spectrometer operating at 22.6 MHz, equipped with an external time-shared ^{19}F field-frequency stabilizer, a quadrature detector, and a Nicolet 1080 data system.[12] A ^{13}C insert accepting 10-mm tubes was used with the ^{13}C coil wound on the inside of a 13-mm glass coil support and the ^{1}H coil wound on the outside, approximately orthogonal to both H_0 and the ^{13}C coil. Power amplifiers capable of 200 W continuous wave were used for both ^{13}C and ^{1}H channels, producing a maximum $(H_1)_{proton}$ of 10 G and an $(H_1)_{carbon}$ four times that.

Matched spin-lock (SL), single-contact cross-polarization, or Hartmann–Hahn experiments were performed using a four-part procedure.[4] First, the proton spins were polarized in H_0. Then they were placed in the rotating frame by a 90° pulse followed by a 90° phase shift and continuous application

of a strong ^1H rf field. The third part of the experiment was to establish ^{13}C–^1H contact for some variable time by placing the ^{13}C spins into the rotating frame by continuous rf irradiation of the carbon spins such that $\gamma_{carbon}(H_1)_{carbon} = \gamma_{proton}(H_1)_{proton}$. The amplitudes of the two rf fields, $(H_1)_{carbon}$ and $(H_1)_{proton}$, were adjusted with 1 dB precision. The final step was to sample the ^{13}C magnetization by turning off $(H_1)_{carbon}$, but still with dipolar decoupling of the ^1H spins. All CP experiments were performed with alternation of spin temperatures to avoid artifacts.[13]

Adiabatic demagnetization in the rotating frame (ADRF) was achieved by first spin locking the protons as described above and then, in times on the order of 1–10 ms (long compared to the proton T_2), reducing $(H_1)_{proton}$ to zero by means of an analogue-controlled, nonlinear rf gate driven by the ramp of a waveform generator, the latter operating in a single-shot, externally triggered mode. The turnoff curve of $(H_1)_{proton}$ was approximately S shaped, with the time constants for the initial and intermediate sections separately adjustable. Following ADRF of the protons, CP contact was made between the protons (now spin-locked along their local field) and the carbons by turning on an $(H_1)_{carbon}$ greater than the local field for a variable time, generally on the order of 1–10 ms. The final step of the ADRF experiment was to sample the ^{13}C magnetization by turning off $(H_1)_{carbon}$, simultaneously turning on $(H_1)_{proton}$ in order to obtain a dipolar-decoupled ^{13}C free induction decay. Successful ADRF experiments performed on adamantane[14] (in which considerably more polarization was transferred per contact than in SL experiments) confirmed that the adiabatic demagnetization of the protons was reasonably effective.

(B) The ^{13}C $T_{1\rho}$ Experiment. The lifetime of the carbon magnetization in its rotating field, $(H_1)_{carbon}$, was measured using the procedure shown in Figure 1. A carbon magnetization was first established by a CP procedure. Contact was then broken between protons and carbons, usually by simply rapidly turning off $(H_1)_{proton}$, but occasionally (for reasons to be discussed in section VB) with a more elaborate "spoil" sequence consisting of repetitive 90° pulses. The carbon spins were then held in their rotating field for a variable time, after which the remaining ^{13}C magnetization was sampled with dipolar decoupling of the protons. The time constant for the decay process of the ^{13}C magnetization along $(H_1)_{carbon}$ during the "hold" period is the ^{13}C $T_{1\rho}$. The carbon $T_{1\rho}$ can be determined by either the spin–spin or the spin–lattice processes, or a combination of both. (This situation will be discussed in section V.)

(C) Source of Polymers. All of the polymers used in this study were commercial plastics. They were obtained from their manufacturers as high molecular weight materials, free from additives such as plasticizers or rubber fillers. The polymers were poly(methyl methacrylate) (Rohm and Haas), polycarbonate (General Electric), poly(phenylene oxide) (General Electric), polystyrene (Monsanto), polysulfone (Union Carbide), poly(ether sulfone) (Imperial Chemicals Industry, UK), and poly(vinyl chloride) (Monsanto). The poly(phenylene oxide) and poly(vinyl chloride) samples were obtained from their respective manufacturers on a special request basis to avoid the additives normally found in the commercially available products. Intrinsic viscosity measurements confirmed the high molecular weights of all the materials. Carbon-13 spectra of the polymers in suitable solvents confirmed the absence of significant concentrations of additives, residual monomer, etc.

Solid plugs of each polymer were compression molded well above T_g using a 6-in. air cylinder exerting approximately 10 000 psi on a 10-mm diameter stainless steel ram. These plugs were 9-mm in diameter by 20 mm in length. The temperature of the mold was lowered from above T_g to room

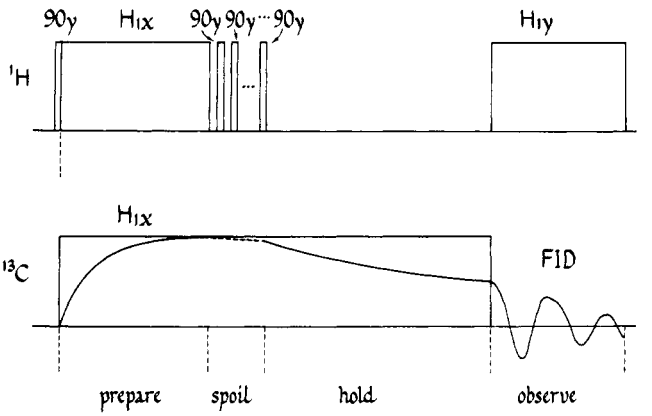

Figure 1. Pulse sequence for the ^{13}C $T_{1\rho}$ experiment. The first part of the experiment is a matched Hartmann–Hahn CP preparation of carbon magnetization. The second part (the "spoil" sequence of 90° pulses separated by ^1H T_2's) is usually omitted; it is included only when searching for possible effects of transients in the ^1H channel on the ^{13}C channel. The third part of the experiment is the variable time the carbons are held in their rotating frame without CP contact with the protons. This is followed in the fourth part by the observation of the carbon free induction decay with resonant dipolar decoupling of the protons.

temperature in less than 15 min. The resulting materials were considered quenched, glassy polymers, and, with one exception, displayed x-ray diffraction patterns consistent with completely amorphous materials. The exception was poly(phenylene oxide), whose x-ray diffraction pattern and heat of fusion suggested the possibility of a crystalline component[15] comprising on the order of 20–30% of the sample. For our purposes, we consider even this polymer predominantly amorphous in character.

Several annealed[16] plugs of polycarbonate were prepared by holding quenched samples in an oven at 135 °C, some 15 °C below the glass transition temperature, for 20 days.

(D) Construction and Operation of Magic-Angle Rotors. Rotors were machined from solid polymer plugs using a Maximat V10P, 10-in. swing, bench metal lathe and milling machine (American Edelstaal). The proportions of the rotor, axle support, and driving gas jet have been illustrated before.[17] The overall dimensions of the rotor and support were such that they fitted an NMR probe designed for 10-mm diameter sample tubes. The volume of the rotor was about half of the effective sample volume that is realized by filling a 10-mm thin-wall NMR tube with a solid polymer plug, having a height equal to that of the ^{13}C receiver coil. (Spectra of nonspinning samples were usually obtained using such solid plugs.)

In the construction of the rotors, considerable care was taken to ensure that the mass of the rotor was symmetrical about the axis defined by the axle holes. Once up to their operating speeds, the rotors spun without detectable vibration and virtually without wear. Some of the rotors used in this study were spun for more than 20 h without significant signs of wear. This result suggests that the rotors generate their own frictionless air bearings, a notion supported by the fact that from zero to 3.2 kHz the spinning speed of the rotors was proportional to the pressure of the driving nitrogen gas. Occasionally a rotor failed by wearing, fatiguing, and breaking an axle. These failures were rare, did no damage to the insert, and did not constitute a safety hazard.

Since H_0 and the magic-angle rotational spinning axes were both horizontal, the magic angle was achieved by rotating the support about a vertical axis. This was facilitated by making that part of the spinner support that remained outside of the probe of such shape and dimensions that it only fit between the pole faces of the magnet when the orientation was correct.

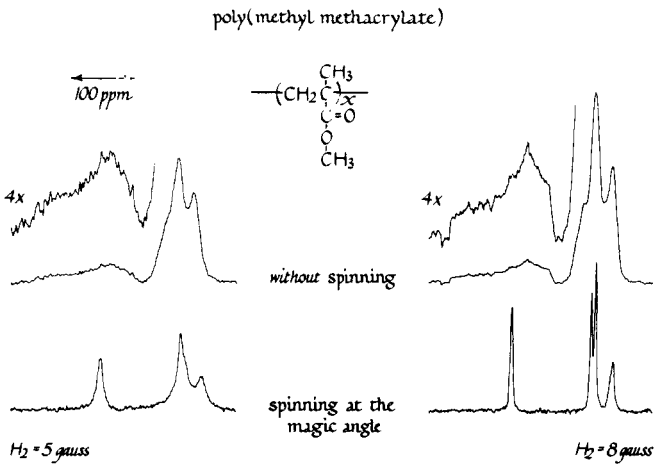

Figure 2. Cross-polarization ^{13}C NMR spectra of poly(methyl methacrylate), with and without magic-angle spinning at 3 kHz, for two values of the decoupling field.

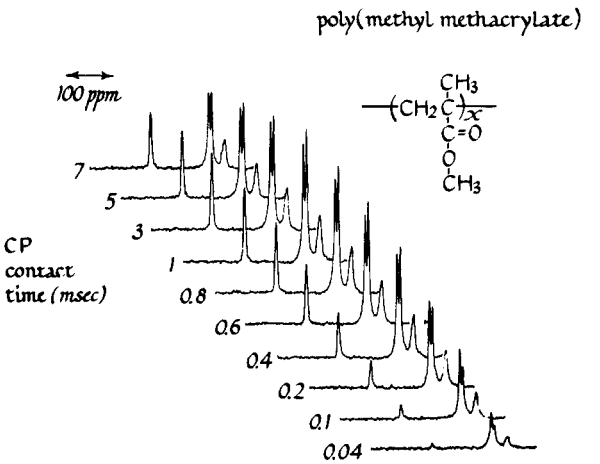

Figure 3. Magic-angle CP ^{13}C NMR spectra of poly(methyl methacrylate) as a function of contact time.

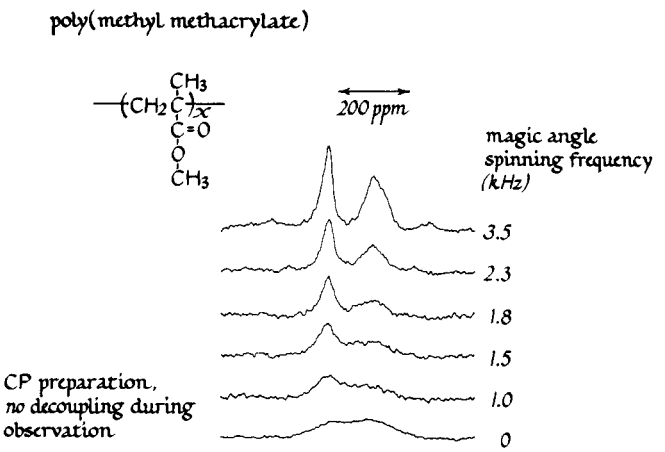

Figure 4. Magic-angle CP ^{13}C NMR spectra of poly(methyl methacrylate) as a function of spinning frequency. Resonant dipolar decoupling has been omitted. Only the two nonprotonated carbon lines are narrow enough to be observed easily.

The remaining play in the support assembly permitted the final fine adjustment to ±1° of the magic angle (54.7°).

(E) Impact Strength Measurements. Impact strengths were measured at room temperature using a conventional notched Izod test, in which a weighted pendulum dropped from a fixed height onto an 0.3-cm thick specimen containing a notch with a 0.03 cm notch radius. The samples were sufficiently thin that, for example, polycarbonate always failed in a ductile manner. The Izod test was repeated some 10–20 times, and the appropriate statistics were performed.

III. Results

(A) Poly(methyl methacrylate). The ^{13}C CP NMR spectra of poly(methyl methacrylate), both with and without magic-angle spinning, are shown in Figure 2, for two values of $(H_1)_{proton}$, designated in the figure as H_2, the dipolar decoupling field. The line assignments for this polymer have been given before.[1] In order of increasing magnetic field, from left to right, the lines in the magic-angle CP spectrum obtained with the higher decoupling field are assigned to the carboxyl carbon, the ester-methyl carbon, and the quaternary carbon, with the highest field line assigned to the α-methyl carbon. The methylene-carbon line is somewhat broader than either of the methyl-carbon lines and is predominantly, but not exclusively, underneath the ester-methyl carbon line. The position of the methylene-carbon line can be inferred from the line shape of the central grouping in cross polarization experiments utilizing short contact times (cf., below). The relative intensities of the carbonyl-carbon line, the central group of lines, and the high-field α-methyl carbon line are 1, 3, and 1, respectively. The α-methyl carbon resonance is somewhat asymmetric, even under magic-angle spinning conditions, due to a dispersion of isotropic shifts arising from stereochemical differences within the chain.[18] These shifts are not quite resolved.

Comparison of the CP spectra obtained with 5 G ($\gamma H_2/2\pi$ = 20 kHz) decoupling to those obtained with 8 G decoupling shows that no residual dipolar broadening is being removed by the 3-kHz spinning. Both spinning and nonspinning spectra are broadened to the same extent (Figure 2). Since protonated carbon lines are broadened only slightly more than nonprotonated carbon lines, it is clear even the lower decoupling field is reasonably effective and all protons are being stirred. Residual dipolar broadening is minor.

In a general sort of way, the line narrowing achieved by the magic-angle spinning appears to be remarkably good. That is, even though the 3-kHz spinning frequency is just greater than the anisotropic dispersion of chemical shifts for, say, the carbonyl-carbon line of poly(methyl methacrylate) shown in Figure 2, this line is narrowed by a factor of 35.

The buildup of carbon magnetization as a function of spin-lock CP contact with polarized protons is shown for poly(methyl methacrylate) in Figure 3. These spectra were taken with magic-angle spinning and are directly comparable to spectra of the same polymer obtained under nonspinning conditions, presented earlier.[1] The two sets of results are similar. The carbonyl-carbon line builds up most slowly and the relatively broad methylene-carbon line most rapidly. Magic-angle spinning increases the time constant describing the carbonyl-carbon polarization in these experiments by much less than a factor of 2; spinning has no detectable effect on the time constant associated with the methyl- and methylene-carbon cross-polarization. After about 3-ms CP contact, the intensity of all the carbon lines decreases. The time constant describing this decay is the proton $T_{1\rho}$, which, for poly(methyl methacrylate) at room temperature, is about 7 ms.

Figure 4 shows the results of some *single*-resonance CP magic-angle spinning experiments on poly(methyl methacrylate). These experiments were performed in the usual way, preparing a carbon magnetization by a matched Hartmann–Hahn CP transfer, except that the carbon free induction decay was obtained without resonant dipolar decoupling. The only lines narrow enough to be easily observed arise from the two

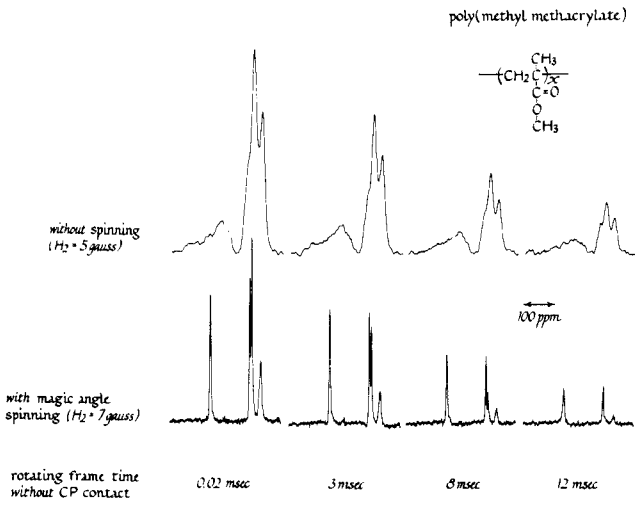

Figure 5. Cross-polarization ^{13}C NMR spectra of poly(methyl methacrylate), with and without magic-angle spinning, as a function of the time the carbon magnetization was held in the rotating frame without CP contact. The relaxation rates are characterized by ^{13}C $T_{1\rho}$'s.

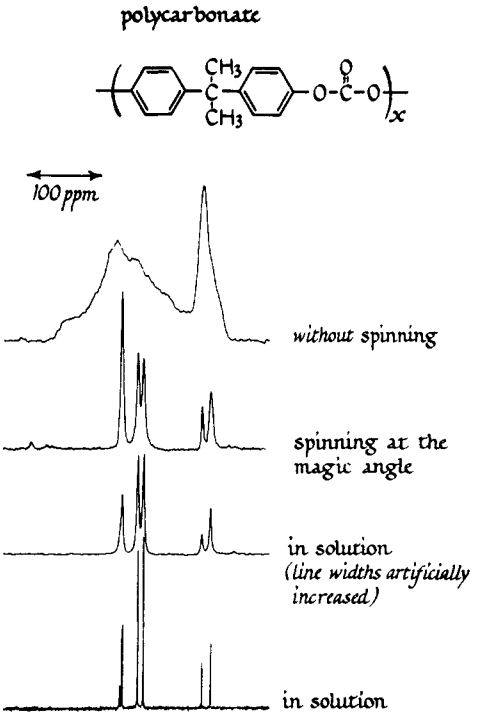

Figure 6. Cross-polarization ^{13}C NMR spectra of polycarbonate, with and without magic-angle spinning. The CP spectra are compared to a FT spectrum of the polymer in solution (with solvent lines omitted for clarity of presentation). The FT spectrum is not fully relaxed.

nonprotonated carbons. As the spinning frequency is increased, a modest narrowing of these lines by a factor of about 3 is observed. There is no loss in intensity of either line with increasing spinning frequency. (The spectrum obtained at zero spinning frequency has a better signal-to-noise ratio because four times as many transients were accumulated.)

The results of some $T_{1\rho}$ experiments (as outlined in Figure 1 but *without* the "spoil" sequence) on poly(methyl methacrylate) are presented in Figure 5. The spectra of the nonspinning system clearly show (from integrated intensities) that the carbonyl-carbon line is relaxing at a much slower rate than the high-field group of lines. There is a small variation in relaxation rate across the carbonyl-carbon chemical shift dispersion. Furthermore, from changes in the line shape patterns of the high-field group, it is clear that some differential relaxation is also occurring there. However, a straightforward interpretation of the changing patterns in the high-field grouping is not possible. In general, the overlapping chemical shift anisotropies are not subject to a simple, computer-assisted spectral decomposition, as overlapping lines often are in the FT spectra of polymer solutions.

The confusion is, however, totally removed by performing the $T_{1\rho}$ experiment while spinning the polymer at the magic angle (Figure 5). The time constants describing the decays of each of the lines are the ^{13}C $T_{1\rho}$'s. Completely unexpected details of relaxation patterns become immediately obvious from these magic-angle spectra. For example, by comparison of Figures 3 and 5, the quaternary-carbon line has a short $T_{1\rho}$ even though possessing one of the longest T_{CH}(SL). None of the observed $T_{1\rho}$ relaxation patterns is a strong function of either the choice of $(H_1)_{carbon}$ or the magic-angle spinning frequency.

(B) Polycarbonate. The ^{13}C CP NMR spectra of polycarbonate, both with and without magic-angle spinning, are compared to the standard FT NMR spectrum of the polymer in solution in Figure 6. Line assignments are straightforward. From the spectrum of polycarbonate in solution, the weak, lowest field line can be assigned to the carboxyl carbon. (This line is not fully relaxed.) A closely spaced pair of lines, which can be assigned to the four nonprotonated aromatic carbons, appear at slightly higher field. A somewhat more widely spaced pair of lines of greater intensity appear at still higher field, and these are assigned to the eight protonated aromatic carbons of the repeating unit. No attempt will be made to distinguish between different types of nonprotonated or between different types of protonated aromatic carbons. (As we shall see, there are no important differences in relaxation behavior for lines within a given carbon classification.) Two lines are observed at substantially higher field, with the more intense of the two assigned to the methyl carbons of the polycarbonate repeat unit, and the other to the quaternary carbon.

The magic-angle CP and the solution FT spectra (the latter with a suitable line broadening function added) are similar, but not identical. Some differences in relative intensities are observed, due primarily to the fact that the FT spectrum is only partially relaxed. Two more interesting differences are first, that some spinning side bands are observable in the magic-angle CP spectrum of the solid, and second, that the methyl-carbon line width in the CP spectrum is about twice as great as that of the quaternary carbon, and about 50% greater than that of the protonated aromatic-carbon line widths. Unfortunately, even with spinning, the resolution of the polycarbonate spectrum is not quite good enough to distinguish the carboxyl-carbon resonance as a separate line. However, the low-field tail of the CP spectrum of the nonspinning solid can be attributed exclusively to the carboxyl carbon since this tail is absent in the spectra of similar polymers not containing a carboxyl carbon.

This last fact is useful in describing the FT spectra of solid polycarbonate (Figure 7). These spectra were obtained with gated dipolar decoupling both with and without a low-level ^1H continuous-wave irradiation. Comparison of the two spectra permits an evaluation of the nuclear-Overhauser enhancement[8] (NOE) which varies substantially over the polycarbonate line width.[19] The low-field tail, which as mentioned above can be associated with the carboxyl-carbon resonance, shows a substantial NOE of well over 2.0. The center of the spectrum, associated primarily with the aromatic-carbon resonances, shows a modest NOE of about 1.2. The high-field

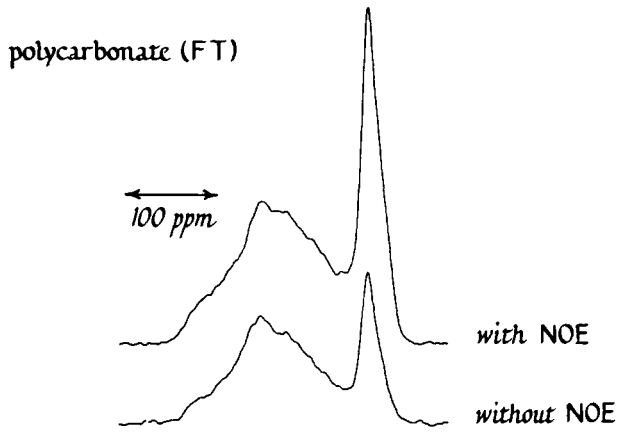

Figure 7. Fourier-transform gated dipolar-decoupled ^{13}C NMR spectra of polycarbonate, with (upper) and without (lower) low-level continuous wave rf irradiation of protons.

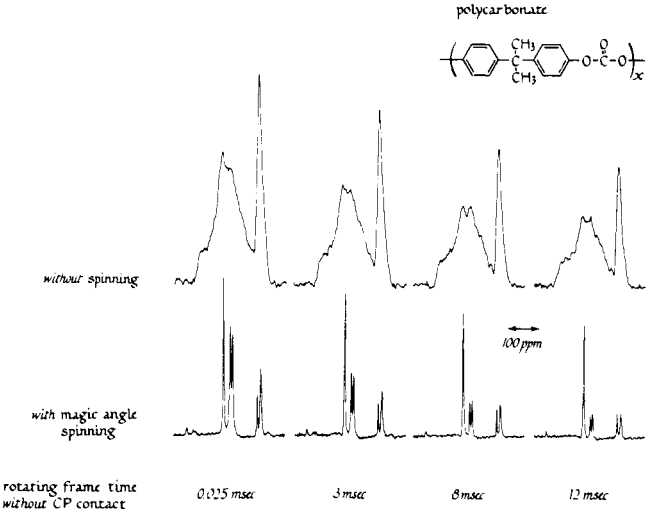

Figure 8. Cross-polarization ^{13}C NMR spectra of polycarbonate with and without magic-angle spinning as a function of the time the carbon magnetization was held in the rotating frame without CP contact.

line, which is mostly, but not exclusively, due to the methyl carbons, has a large NOE approaching 2.5.

As was the situation with poly(methyl methacrylate), the results of ^{13}C $T_{1\rho}$ experiments are far more informative when performed under magic-angle spinning conditions (Figure 8). Except for some quite minor variation in relaxation behavior across the polycarbonate line shape, as well as the relaxation behavior of the low-field carboxyl shoulder and that of the high-field methyl-carbon peak, there is little detail in the $T_{1\rho}$ experiment on the nonspinning solid. With magic-angle spinning, however, the relatively fast relaxation of the protonated carbons is readily apparent. The $T_{1\rho}$ relaxation of the lines arising from the nonprotonated carbons of polycarbonate is slower than that of the protonated aromatic carbons even though both kinds of carbons necessarily share the same motions. This behavior simply reflects the weaker coupling of nonprotonated carbons to more distant protons as determined by the inverse sixth power dependence on the internuclear separation common to all dipolar interactions.

A semilog plot of the protonated aromatic-carbon magnetization of polycarbonate as a function of the CP Hartmann–Hahn contact time is shown in Figure 9. This is a graphic presentation for one of the carbons of polycarbonate of the results of a series of experiments similar to those shown

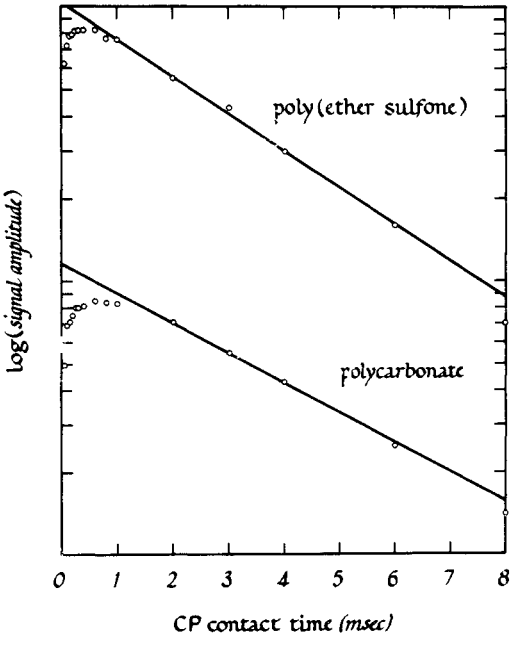

Figure 9. Plots of the protonated aromatic-carbon intensities as a function of CP contact time (with magic-angle spinning) for polycarbonate and poly(ether sulfone).

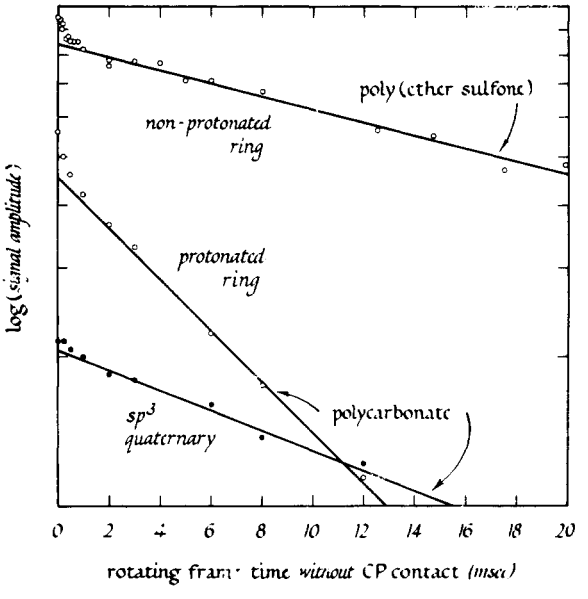

Figure 10. Plots of various magic-angle CP ^{13}C NMR signal intensities as a function of the time the carbon magnetization was held in the rotating frame without CP contact.

in Figure 3 for poly(methyl methacrylate). The average rate of change over the first 50 μs of this plot is taken as the average T_{CH}(SL). Determination of this value for amorphous polymers is not complicated by pronounced transient oscillations, as is sometimes the situation in crystalline materials.[5,20] The final slope yields the proton $T_{1\rho}$.[5] In general, we find that plots such as those shown in Figure 9, fitted by a sum of exponentials with parameters matched to the initial and final slopes, are only qualitatively represented in the intermediate region.

Figure 10 shows some ^{13}C $T_{1\rho}$ data for polycarbonate, also presented in a familiar semilog fashion. This figure is closely analogous to ordinary T_1 plots[21] describing the spin–lattice relaxation of, say, simple organic molecules in solution. It is

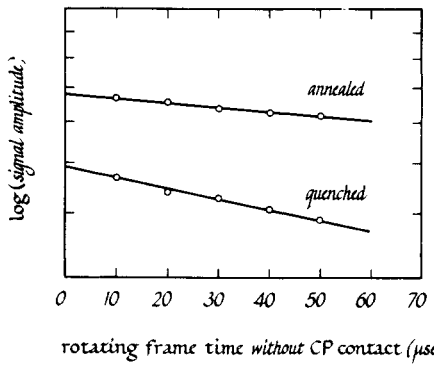

Figure 11. The initial slopes of plots such as those shown in Figure 10 for quenched and annealed polycarbonate. Annealed samples were prepared by holding quenched material at 135° for 20 days.

clear from Figure 10, however, that, in general, ^{13}C $T_{1\rho}$ plots for glassy polymers are not linear, but instead show a dispersion, or distribution of relaxation times, even for a chemically unique carbon giving rise to a single sharp line under spinning conditions. This distribution of relaxation times cannot be explained solely by the distributions of correlation times often invoked to describe relaxation phenomena in polymers.[22] Rather, a distribution of NMR relaxation times such as this suggests a multiplicity of noninterconverting dynamic environments for chemically, or structurally, nearly equivalent carbons.[23]

The ^{13}C $T_{1\rho}$ dispersion is typically different for different polymers and even for different carbons in the same polymer. For polycarbonate, the dispersion is pronounced for both protonated and nonprotonated aromatic carbons but is much smaller for the quaternary and methyl carbons. Thus, in $T_{1\rho}$ experiments in which the ^{13}C rotating frame time without CP contact is short, say 50 μs, a substantial fraction of the protonated aromatic-carbon intensity is lost, while virtually none of the quaternary- or methyl-carbon intensities are lost. The polycarbonate $T_{1\rho}$ dispersions are more pronounced, for example, than those for the methylene carbons of poly(methyl methacrylate). The initial slope of the $T_{1\rho}$ plot for the protonated aromatic carbon of polycarbonate (Figure 11) is 40 times greater than the final slope (Figure 10).

The $T_{1\rho}$ dispersion for the protonated carbons of polycarbonate is reduced, but not eliminated, when the sample is *not* spinning at the magic angle. That is, in experiments similar to those illustrated in the top part of Figure 8, but in which relatively short contact times had been employed, so that the observed carbon magnetization was predominantly due to the protonated aromatic and methyl carbons, the loss of signal intensity after 50 μs in the rotating frame without contact with the protons was only about 20% of what it was in the same experiment but with sample spinning at 3 kHz.

The magic-angle $T_{1\rho}$ dispersion for polycarbonate is affected by annealing of the polymer. Thus, the initial slope (over the first 50 μs) of the $T_{1\rho}$ plot for the protonated aromatic carbon of quenched polycarbonate is greater by a factor of about 2.5 than the corresponding value for an annealed sample (Figure 11). The initial slope of the $T_{1\rho}$ plot yields the average $T_{1\rho}$ (designated $\langle T_{1\rho} \rangle$) for the entire sample. Thus, annealing results in a reduction of the $T_{1\rho}$ dispersion; or, in other words, annealing tends to homogenize the relaxation behavior of polycarbonate as characterized by $T_{1\rho}$. No other differences in relaxation parameters for the two samples were detected. Quenched and annealed polycarbonate had the same T_{CH}(SL), NOE, and proton $t_{1\rho}$, as well as the same final slopes in carbon $T_{1\rho}$ plots, all within experimental error.

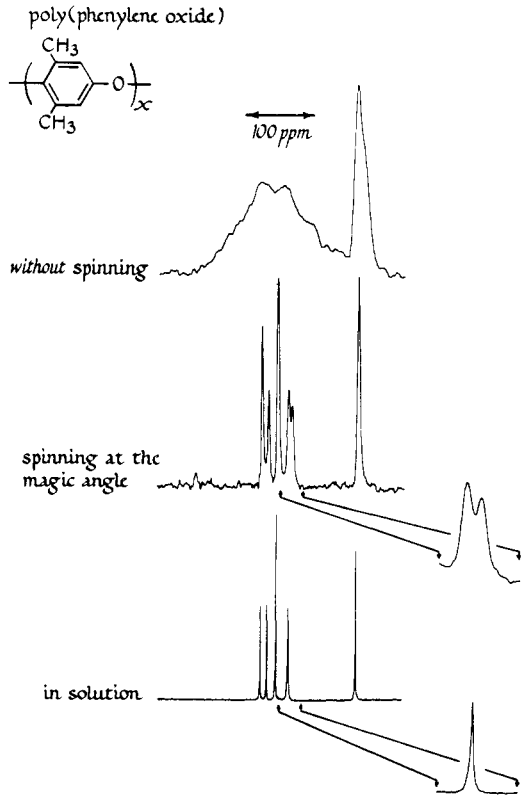

Figure 12. Cross-polarization ^{13}C NMR spectra of poly(phenylene oxide), with and without magic-angle spinning. The CP spectra are compared to a FT spectrum of the polymer in solution (with solvent lines omitted for clarity of presentation).

(C) Poly(phenylene oxide). The ^{13}C CP NMR spectra of poly(phenylene oxide), both with and without magic-angle spinning, are compared to the standard FT NMR spectrum of the polymer in solution in Figure 12. Line assignments can be made on the basis of the relative intensities of the lines in the fully relaxed solution spectrum, as well as characteristic chemical shifts. The two lowest field lines are assigned to the 1,4-quaternary carbons and the double-intensity line to the 2,6-quaternary carbons. The fourth line in the spectrum (in order of increasing magnetic field) is also double intensity, although its greater line width makes a carbon count based on peak height deceptive. This line is assigned to the two protonated aromatic carbons of the repeating unit. The high-field line is assigned to the methyl carbons.

The magic-angle CP spectrum of the solid is substantially different in at least two respects. First, the relative intensities of the CP spectrum differ from those of the fully relaxed FT spectrum, particularly for the low-field quaternary-carbon lines. This is simply a result of the choice of contact time (500 μs) which was not sufficiently long to allow a full CP transfer for all the carbons.[4] (These observed differences in intensity can, in fact, form the basis of a method of making more detailed line assignments than those given above.) Second, and more importantly, the protonated aromatic carbon line, which is a singlet in the solution spectrum, is a doublet in the magic-angle CP spectrum of the solid. The inserts in the figure show expansions of the horizontal scales of the two spectra; the singlet frequency occurs at the center of the doublet.

The results of some ^{13}C $T_{1\rho}$ experiments are shown in Figure 13. As with poly(methyl methacrylate) and polycarbonate, the $T_{1\rho}$ experiment on the nonspinning solid is not particularly revealing. With magic-angle spinning, however, the exceptionally fast relaxation of the protonated aromatic-carbon lines becomes clear. Both parts of the doublet behave the same

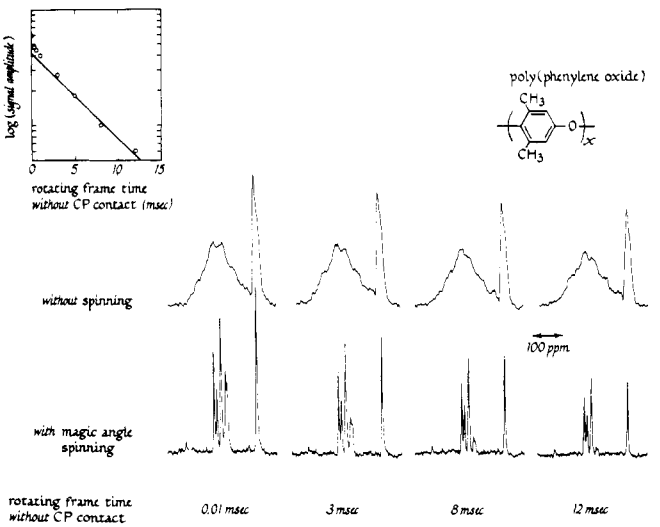

Figure 13. Cross-polarization ^{13}C NMR spectra of poly(phenylene oxide), with and without magic-angle spinning, as a function of the time the carbon magnetization was held in the rotating frame without CP contact. The insert shows the $T_{1\rho}$ relaxation behavior of the protonated aromatic-carbon doublet.

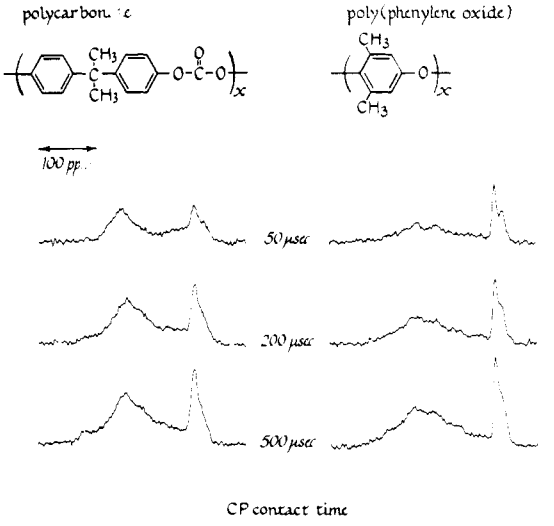

Figure 14. Cross-polarization ^{13}C NMR spectra of polycarbonate and poly(phenylene oxide) obtained using short contact times.

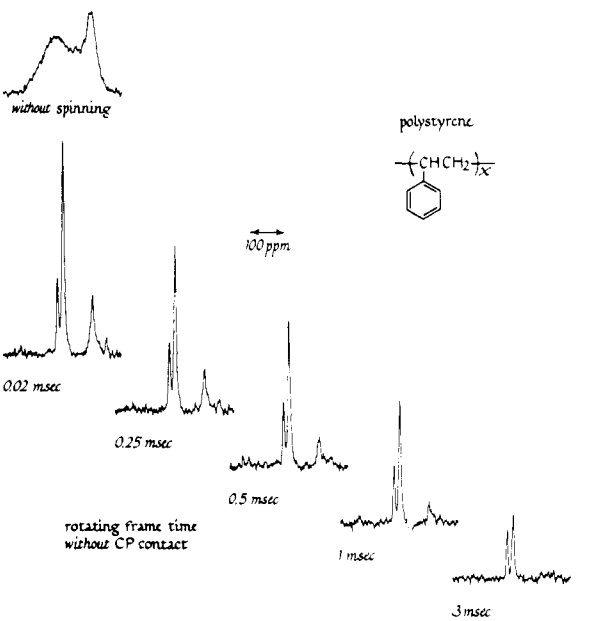

Figure 15. Magic-angle CP ^{13}C NMR spectra of polystyrene as a function of the time the carbon magnetization was held in the rotating frame without CP contact. The insert shows a CP spectrum obtained without magic-angle spinning.

way in this experiment, and both have almost as fast a $T_{1\rho}$ relaxation as, for example, the protonated aromatic carbons of polycarbonate. The remaining carbon lines of poly(phenylene oxide), including the methyl-carbon lines, are relatively slow relaxers. All of the carbon lines of poly(phenylene oxide) have a pronounced $T_{1\rho}$ dispersion. The insert in Figure 13 illustrates the $T_{1\rho}$ dispersion for the protonated aromatic-carbon lines of poly(phenylene oxide). The $T_{1\rho}$ relaxation behavior of the methyl-carbon line has an unmistakable dependence on the magic-angle spinning frequency; the relaxation is faster with 3-kHz spinning than without it.

The methyl-carbon resonance of nonspinning poly(phenylene oxide) has an asymmetry (Figure 13). This asymmetry, arising from chemical shift anisotropy, is altered in CP experiments involving short carbon–proton contact times.[4] In fact, for contact times on the order of 50 μs, a distinct hole appears in the methyl-carbon resonance at its isotropic center (Figure 14). This hole fills in for somewhat longer contact times. A similar, though somewhat less well defined, hole appears in the CP spectra of polycarbonate (Figure 14).

(D) Polystyrene. The ^{13}C CP NMR spectra of polystyrene, both with and without magic-angle spinning, are shown in Figure 15. The spectra of the spinning solid are well enough resolved that the quaternary carbon is easily distinguished from the remaining low-field aromatic-carbon resonances, all of which are grouped in a single intense line. The high-field line arises from the methine and methylene carbons. The remaining lines in the spectrum are spinning side bands. (Note that the spinning side bands of an asymmetric line shape are not equal in intensity.[24]) These spectra are similar to some earlier FT spectra of polystyrene obtained with resonant dipolar decoupling and under magic-angle spinning conditions.[1] The present spectra are of substantially improved quality.

The results of some ^{13}C $T_{1\rho}$ experiments performed on spinning polystyrene are also shown in Figure 15. The main-chain carbon lines are relatively fast relaxers, with most of their signal missing after 3 ms in the rotating frame without CP contact. The quaternary aromatic-carbon line is, on the other hand, a slow relaxer, and the remaining protonated aromatic-carbon line is intermediate. Plots of the $T_{1\rho}$ decays, similar to those shown in Figure 10 for other polymers, establish that $T_{1\rho}$ dispersions are present for all the carbons of polystyrene. However, the dispersion for the aromatic-carbon line is not particularly pronounced relative to that for the main-chain carbon line, which, in turn, displays less of a dispersion than that for the protonated carbon lines of polycarbonate and poly(phenylene oxide).

The effect of variable CP contact times in matched Hartmann–Hahn experiments performed on spinning polystyrene is shown in Figure 16 (bottom). The aromatic quaternary-carbon line, and to a lesser extent, the protonated aromatic-carbon line, increase in intensity for contact times longer than 100 μs. The main-chain carbon line, however, reaches its full intensity before 100 μs. After about 1 ms, all the polystyrene lines decrease in intensity because of the short proton $T_{1\rho}$.

(E) Polysulfone and Poly(ether sulfone). The ^{13}C CP NMR spectra of polysulfone and poly(ether sulfone), both with and without magic-angle spinning, are compared to the standard FT NMR spectra of the two polymers in solution in Figure 17. This figure dramatizes the importance of spinning in interpreting the solid-state ^{13}C NMR spectra of polymers.

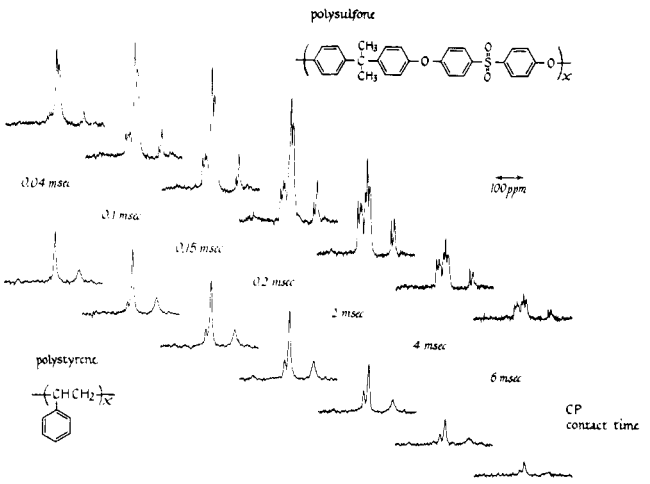

Figure 16. Magic-angle CP ^{13}C NMR spectra of polystyrene and polysulfone as a function of CP contact time.

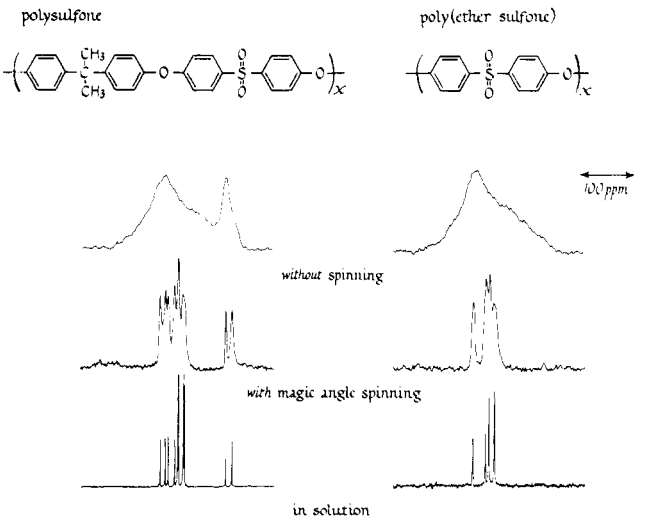

Figure 17. Cross-polarization ^{13}C NMR spectra of polysulfone and poly(ether sulfone), with and without magic-angle spinning. The CP spectra are compared to FT spectra of the polymers in solution (with solvent lines omitted for clarity of presentation). There are ten lines in the FT spectrum of polysulfone and eight in the magic-angle CP spectrum. Spinning sidebands are visible in the CP spectrum of polysulfone.

Except for the high-field line in the spectrum of polysulfone, the CP spectra of the two nonspinning polymers are virtually identical. With magic-angle spinning, however, differences in the aromatic-carbon region are clearly established. In fact, the magic-angle spinning spectra of the solid polymers are almost as detailed as the standard FT spectra of solutions of the two. There are no differences between the bulk and solution isotropic chemical shifts for either polymer.

Partial line assignments for both polymers can be made on the basis of the relative intensities observed in the fully relaxed FT spectra of the polymer solutions (Figure 17). Thus, in both cases, the weaker, lower field lines can be assigned to the non-protonated aromatic carbons, and the more intense, higher field lines to the protonated aromatic carbons. Just as in the situation for polycarbonate, the quaternary-carbon resonance of polysulfone is at somewhat lower field than that of the methyl carbons, which appears at extreme high field. No attempt will be made to make more detailed line assignments, although a wide variety of techniques,[25] developed for solution ^{13}C FT NMR, are available for this purpose and would, for the most part, still be suitable for solids.

The line shapes of both polysulfone and poly(ether sulfone) observed with magic-angle spinning are not simple. In fact, the lowest field line of poly(ether sulfone) is, if sufficient care is taken in adjusting the magic angle, occasionally resolved into a doublet, although the resolution is much poorer than that observed in experiments on poly(phenylene oxide). The highest field line of that polymer also shows some unresolved fine structure. Spectra of poly(ether sulfone) in solution show no fine structure. The methyl-carbon line width of solid polysulfone is about twice that of the quaternary carbon, and both lines appear to be symmetric, or, more accurately, fail to show any unresolved fine structure. The same situation is observed for these two types of carbons in polycarbonate (Figure 6).

A semilog plot of the protonated carbon magnetization of poly(ether sulfone) as a function of the CP Hartmann–Hahn contact time is compared to a similar plot for a comparable carbon of polycarbonate in Figure 9. The transfer of polarization under matched Hartmann–Hahn conditions is, for short contact times of 100 μs or less, more efficient for poly(ether sulfone) than for polycarbonate. There are no indications of transient CP oscillations in Figure 9 for either poly(ether sulfone) or polycarbonate. By coincidence, the proton $T_{1\rho}$'s for the two polymers are just about the same.

The ^{13}C $T_{1\rho}$ dispersions for the protonated aromatic carbons of both poly(ether sulfone) and polycarbonate are qualitatively similar. The $T_{1\rho}$ dispersions for the nonprotonated aromatic carbons of the two polymers are also similar to one another and are, in addition, identical in shape to the protonated carbon counterparts, but with the initial and final slopes reduced by a factor of about 6 (Figure 10).

A display of the CP spectra of polysulfone as a function of matched Hartmann–Hahn contact time makes an interesting point (Figure 16). For highly complicated magic-angle CP spectra, it is possible to considerably enhance the effective resolution by a judicious selection of CP contact time. For example, the CP spectra of polysulfone are much better resolved for contact times of 2–4 ms than they are for contact times of 100–200 μs, even though the total integrated intensities of some of the lines, and perhaps even the entire spectrum, are reduced for the longer contact times. Furthermore, in some situations, it is possible to hold the carbon magnetization in its rotation frame without CP contact, in order to achieve a further enhancement in resolution resulting from differences in relaxation times.

In general, the CP and ^{13}C $T_{1\rho}$ behavior of poly(ether sulfone) and polysulfone are comparable.

(F) Poly(vinyl chloride). Poly(vinyl chloride) is an example of a synthetic polymer for which magic-angle spinning provides no real improvement in resolution. The ^{13}C CP NMR spectra of poly(vinyl chloride), both with and without magic-angle spinning, are shown in Figure 18. The methine-carbon resonance of poly(vinyl chloride) may not contribute to the observed signal, because of line broadening arising from static dipolar interactions with directly bonded chlorines. Although the chemical shift anisotropy has been removed by the spinning, complications due to methlylene-carbon shifts arising from the various stereochemical configurations of atactic poly(vinyl chloride),[26] prevent the improvement in resolution usually realized by spinning. (Similar difficulties have been encountered with other vinyl polymers such as polypropylene and polyacrylonitrile.)

Of course, both CP transfer and ^{13}C $T_{1\rho}$ experiments can still be performed on poly(vinyl chloride). The results of these experiments are not strongly dependent on magic-angle spinning frequency. The experimental CP transfer rates are much the same as those observed for the main-chain carbons of polystyrene. A $T_{1\rho}$ dispersion is also observed for poly(vinyl

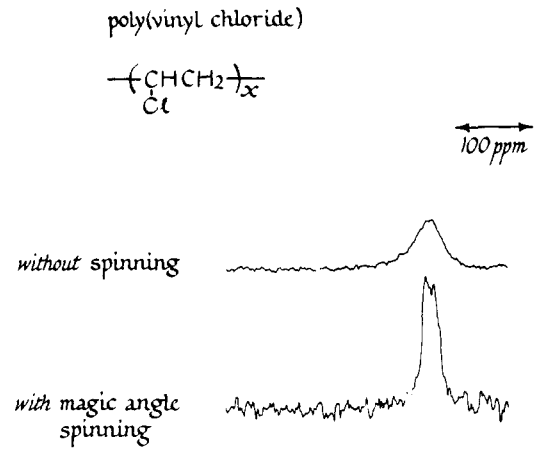

Figure 18. Cross-polarization ^{13}C NMR spectra of poly(vinyl chloride) obtained with and without magic-angle spinning.

chloride) which is somewhat more pronounced than that for polystyrene but generally similar.

(G) ADRF Experiments. The ADRF experiment is not a particularly useful one for glassy polymers near room temperatures. For proton–carbon ADRF contacts less than 1 ms, in experiments performed either on poly(methyl methacrylate) or polycarbonate, there is very little ADRF transfer of polarization. For times on the order of 3 ms, a small transfer is observed. This amounts to less than 10% of the polarization transferred under matched Hartmann–Hahn conditions in 50 μs. For ADRF contact times of 5–10 ms, the net amount of transferred polarization actually decreases from values observed for 3-ms contacts, as the proton lifetime in its local field, T_{1D}, which is comparable to the proton $T_{1\rho}$,[5] is exceeded. Because of the relative inefficiency of the whole process, accurate values of transfer rates are difficult to determine. However, we estimate that T_{CH}(ADRF) for the protonated carbons of poly(methyl methacrylate) and polycarbonate are greater than 50 ms; that is, they are longer than the longest observed, room-temperature, glassy polymer ^{13}C $T_{1\rho}$ by at least an order of magnitude.

(H) Tabulation of NMR Relaxation Parameters and Mechanical Impact Strengths. The average values of T_{CH}(SL) and ^{13}C $T_{1\rho}$ (designated with brackets) obtained for each polymer are presented in Table I. These values were obtained from the average rates of change over the first 50 μs of matched Hartmann–Hahn CP transfer plots and from the initial slopes (averaged, for reasons of sensitivity, over the first 100 μs) of ^{13}C $T_{1\rho}$ plots, respectively. Table I also contains the results of the Izod impact tests.

Table I
^{13}C Relaxation Parameters for Protonated Main-Chain Carbon Lines of Some Glassy Polymers [a,b]

Polymer	$\langle T_{CH}\rangle$, μs	$\langle T_{1\rho}\rangle$, ms	$\langle T_{CH}^{+}\rangle/\langle T_{1\rho}\rangle \times 10^3$	Impact strength, ft lb/in. notch
Polycarbonate	85	0.6	140	14.0
Poly(phenylene oxide)	65	0.9	70	5.0
Polysulfone	75	1.5	50	1.0
Poly(ether sulfone)	55	1.3	40	1.3
Poly(vinyl chloride) (unmodified)	20	0.4	25	0.5
Polystyrene	20	0.8	12	0.3
Poly(methyl methacrylate)	15-20	1.5	10	0.3

[a] Protonated aromatic carbon lines are used for poly(aryl ethers); methylene-carbon line for poly(methyl methacrylate) and poly(vinyl chloride); composite methine- and methylene-carbon lines for polystyrene. [b] $\langle T_{CH}^{+}\rangle = \langle T_{CH}\rangle$/(relative ^{1}H–^{1}H dipolar interaction); relative ^{1}H–^{1}H dipolar interaction is 2 for poly(vinyl chloride) and polystyrene and 1 for all other polymers.

IV. Magic-Angle Spinning, Line Narrowing, and CP Dynamics

On examining magic-angle CP spectra of polymers such as those presented in Figure 2, it is reasonable to ask two general questions: (a) why is the resolution as good as it is despite spinning frequencies which are only slightly greater than the chemical shift dispersion; and (b) why do nonprotonated carbons, such as carbonyl carbons, give rise to strong CP signals even though the spinning frequency would appear to be great enough to eliminate, by motional averaging, the relatively weak ^{1}H–^{13}C static dipolar interactions necessary for a CP transfer of polarization from nonbonded protons to carbons?

(A) Line Narrowing. Magic-angle spinning at modest frequencies is effective in operating on the chemical shift anisotropy because first, there are no long tails to the line shape and second, the chemical shift dispersion is totally static in origin. As shown in the vertical expansion of the carbonyl-carbon resonance of poly(methyl methacrylate) (Figure 2, upper right), the experimental line shape has an abrupt termination. The theoretical line shape is, of course, tentlike with vertical sides, defining the principal values of the chemical shift tensor, σ_{xx}, σ_{yy}, and σ_{zz}.[4,27] Thus, even though the 3 kHz of the magic-angle spinning is just greater than the static shift dispersion, $[\Delta\sigma = \sigma_{zz} - \frac{1}{2}(\sigma_{xx} + \sigma_{yy})]$, in theory there simply are no spectral frequency components, from any source greater than 3 kHz to produce either significant sidebands, or a residual line-broadening effect.

In practice, some line broadening remains. This broadening arises from two sources, both dipolar in origin. The first is associated with dipolar interactions characterized by intermediate correlation frequencies which are not only greater than the magic-angle spinning frequency but are also greater than the frequency of the resonant dipolar decoupling rf field. These intermediate-frequency motions are still sufficiently slow, however, that motional averaging of dipolar interactions is not complete.[1] The residual dipolar broadening therefore depends on the details of the segmental motions of the polymer chain and so will vary from polymer to polymer. Surprisingly, residual broadening from this source is not severe. For the seven glassy polymers studied in detail in this paper, there are apparently only a few, large-amplitude (solid angles greater than ±5%), torsional chain motions having effective correlation frequencies on the order of 10^5 Hz (cf., section VID).

The second source of broadening arises from the fact that the amplitudes of the dipolar decoupling fields are greater, but not much greater, than the proton line widths at room temperature. Thus, some minor broadening remains because the averaging achieved from rf stirring of the ^{1}H spins is not complete (Figure 2). We expect that improvements in resolution, achieved by a combination of magic-angle spinning and dipolar decoupling, can be obtained for polymers such as these by simply increasing the decoupling power (which will remove broadening from both of the sources mentioned above) and making the adjustment of the magic angle itself accurate to better than the present ±1°. The latter becomes important in reaching resolution better than 20 Hz, or 1% of the typical

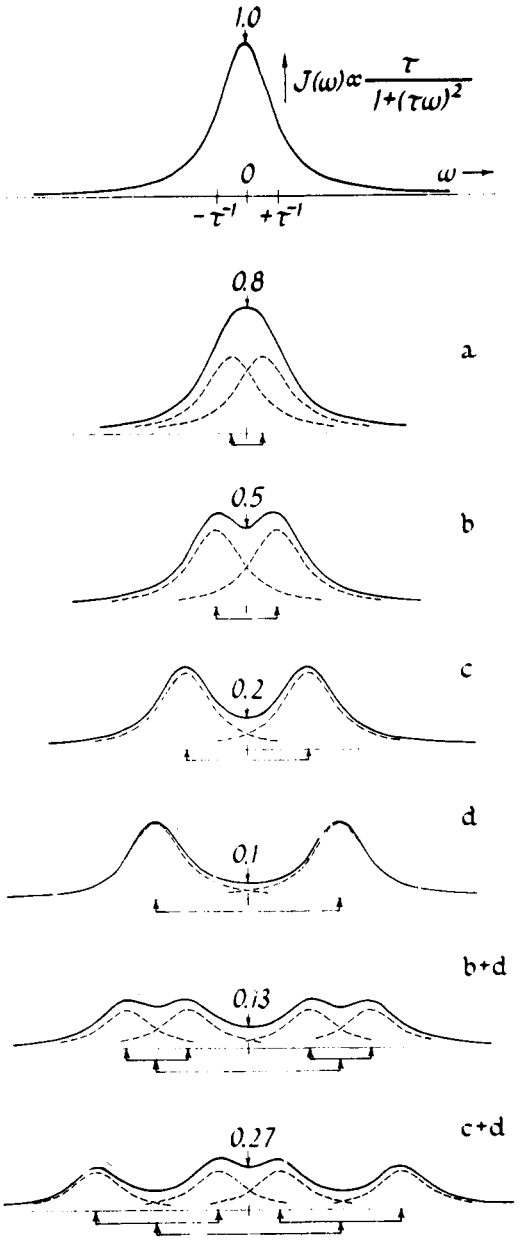

Figure 19. A schematic representation of the effect on the spectral density, $J(\omega)$, of modulation by a variable frequency (a–d) and by two frequencies (b+d, c+d).

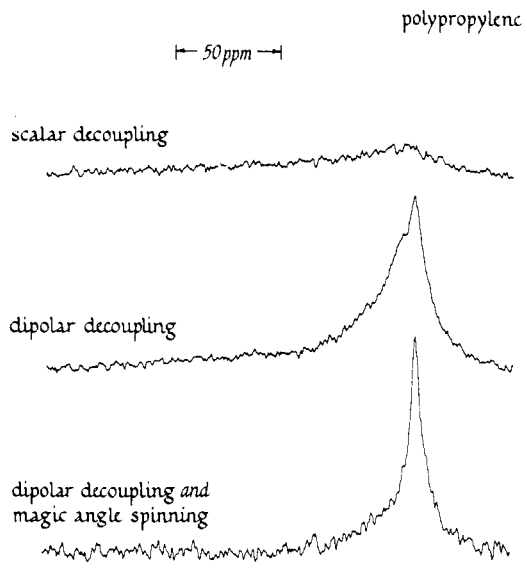

Figure 20. Fourier-transform ^{13}C NMR spectra of polypropylene obtained with scalar decoupling, with dipolar decoupling and with a combination of dipolar decoupling and magic-angle spinning. The resolution of the high-field methyl carbon improves slightly in the combination expement, while the resolution of the rest of the spectrum is degraded.

chemical shift anisotropies.[2] Resolution of better than 50 Hz, however, may never be realized for amorphous polymers, even with efficient decoupling and magic-angle spinning. The ultimate resolution is probably limited by dispersions of isotropic chemical shifts arising from differences in shielding associated with steric and conformational isomerism. For example, it is clear that dispersions of isotropic shifts give rise to the skewing (and so determine the resolution) of the α-methyl carbon line of poly(methyl methacrylate) (Figure 2). We will consider other examples of this behavior in section VIC.

An undesirable factor to consider in the use of a combination of line narrowing techniques is that they can be self-defeating. This situation occurs, for example, when the spinning and rf decoupling field frequencies are comparable to one another.[28] As illustrated in Figure 19a,b, spectral density associated with a nonstatic ^1H–^{13}C dipolar interaction is essentially unaffected by either spinning or decoupling frequencies less than the effective dipolar correlation time, τ. Sidebands are produced on the spectral density and $J(0)$ is reduced as the line-narrowing frequency is increased (Figure 19c,d). (For simplicity, only the first sideband is shown, even though a complicated pattern of higher frequency sidebands is generated.) A combination of line-narrowing techniques, however, produces a second set of sidebands which can return spectral density to zero frequency and so increase residual broadening.[28] The practical point is that one should choose as low a spinning frequency as is consistent with the removal of the chemical shift anisotropy (and its sidebands) in order to obtain the maximum line-narrowing effect of the resonant decoupling.

An example of self-defeating line narrowing schemes is shown in Figure 20. With 4-G decoupling ($\gamma H_2/2\pi$ = 16 kHz) both the main-chain and methyl-carbon lines from the amorphous phase of a solid polypropylene can be observed in an FT experiment. The main-chain carbon line is broad and appears as a low-field shoulder on the methyl-carbon line. (Carbons in the crystalline phase are not decoupled and so not observed.) The residual dipolar broadening is substantial, especially for the main-chain line, and obscures the chemical shift anisotropies for all types of carbons. Considering the segmental mobility of the rubbery, amorphous phase of polypropylene,[29] the residual broadening is probably due to dipolar interactions associated with a wide variety of segmental motions, many of them characterized by effective correlation times on the order of 10^4–10^5 Hz. The dipolar spectral density in this situation can be represented by the plot in Figure 19d. Magic-angle spinning at 3-kHz not only fails to produce any significant narrowing of the methyl-carbon resonance, it appears to broaden and obscure the methylene-carbon resonance. The dipolar spectral density in the combination experiment can be represented by something similar to the plot in Figure 19b+d. This plot has more spectral density near zero frequency than that of Figure 19d. Presumably, correlation frequencies associated with some of the main-chain motions of polypropylene are such that 16-kHz dipolar decoupling is just begining to remove their broadening effect by removal of spectral density from near-zero frequency. Magic-angle spinning at 3 kHz tends to return this spectral

density and so increases the threshold amplitude of the decoupling field necessary for observable narrowing.

(B) CP Dynamics. The chemical shift anisotropy of the quaternary carbon of poly(methyl methacrylate) is sufficiently small that the single-resonance, undecoupled line width of about 4 kHz (Figure 4) can be attributed to ^{1}H–^{13}C dipolar interactions. Room-temperature dipolar line widths of 3–4 kHz are typical for nonprotonated carbons in solid amorphous polymers. These lines narrow by only a factor of 2–4 under 3-kHz magic-angle spinning. This narrowing is far less than that observed for combination spinning and dipolar decoupling experiments. Part of the failure of spinning to narrow more completely the *un*decoupled line is due to the spinning speed being somewhat less than ^{1}H–^{1}H dipolar fluctuations, while part is due to dipolar interactions arising from segmental motions of the polymer having correlation frequencies on the order of 10 kHz. (Broadening due to the latter is not removed by spinning at 3 kHz but is removed by resonant dipolar decoupling at 30 kHz.) In the former situation, substantial spectral density associated with ^{1}H–^{13}C dipolar interactions modulated by rapid ^{1}H–^{1}H dipolar fluctuations remains at zero frequency[28,30] under magic-angle spinning at 3 kHz. This is consistent[31] with the observation that the spin-lock T_{CH}'s for quaternary carbons in amorphous polymers (which are on the order of 300 μs at room temperature) increase by less than a factor of 2 under spinning conditions. Similarly, there is no substantial effect of spinning on protonated carbon T_{CH}'s. Thus, it is possible to think of the survival of the effectiveness of spin-lock CP transfers for all types of carbons in these particular polymer systems at room temperature as due to the inability of low-speed spinning to have much of an effect on the strong ^{1}H–^{1}H dipolar interactions.[31]

V. Carbon-13 $T_{1\rho}$ and Molecular Motion in Solid Polymers

(A) Carbon-13 $T_{1\rho}$ as a Spin–Lattice Relaxation Parameter. Polarization can be transferred between carbons and protons via their mutual static, or near static, dipolar interactions. When both types of spins are locked along their own rotating rf fields, with amplitudes matched according to the Hartmann–Hahn prescription, the time constant for the transfer is $T_{CH}(SL)$.[30] If both rf fields are left on, but the amplitudes are mismatched, $T_{CH}(SL)$ is increased as the transfer is made less efficient.[5] Various aspects of these CP processes have been illustrated and discussed in the earlier sections of this paper.

A new situation arises if one of the rf fields is turned off completely. Transfer of magnetization from a polarized species to an unpolarized species is still possible. The transfer can be that which occurs, for example, between polarized protons which have been adiabatically demagnetized in the rotating frame (so that the dipolar order is preserved along the local field even though the proton rf field has been turned off) and unpolarized carbons in the presence of a strong carbon rf field. The time constant for this spin–spin transfer is designated $T_{CH}(ADRF)$.[5,30] This constant depends upon both secular and nonsecular components of the Hamiltonian associated with ^{1}H–^{1}H dipolar fluctuations.[4,5] This time constant also describes the transfer of magnetization from carbons spin-locked by a strong ^{13}C rf field to abundant *un*polarized protons in the absence of an ^{1}H rf field. The differences between SL and ADRF CP transfer processes have been extensively discussed from both experimental and theoretical standpoints.[5,30]

These discussions have not, however, specifically included organic glassy polymer systems near room temperature. Such polymers are unique solids. In addition to possessing many of the physical characteristics associated with the inorganic solid state, they also are capable of a wide variety of microscopic, or molecular, side- and main-chain segmental motions, even at temperatures well below their glass transitions.[9] This behavior does not occur for inorganic glasses. Some of the polymer main-chain motions are known to occur at frequencies comparable to the ^{13}C rf field.[9] This means the time constant characterizing the lifetime of the carbon spins in their rotating frame may not be dominated by spin–spin processes, described by some sort of $T_{CH}(ADRF)$, but rather may be determined by rotating-frame, spin–lattice, or motional processes. In this situation the same types of molecular motions which are known to be the source of spin–lattice relaxation for the familiar proton $T_{1\rho}$[10,11] will also be responsible for determining the ^{13}C $T_{1\rho}$.

We now present the evidence supporting the conclusion that at room temperature, for glassy polymers, the ^{13}C $T_{1\rho}$ is dominated by spin–lattice-like processes and hence is sensitive to those motions of the polymers having frequencies comparable to the applied carbon rf field.

(1) The experimentally observed $T_{CH}(ADRF)$'s (for $(H_1)_{carbon}$ = 32 G) are about one order of magnitude longer than the longest observed ^{13}C $T_{1\rho}$ and almost three orders of magnitude longer than the shortest $T_{1\rho}$. Theoretically, if the ^{13}C $T_{1\rho}$ were at its minimum value for a protonated methine carbon, a value approximately three orders of magnitude less than the minimum T_1 would be observed.[11] This amounts to something on the order of 50 μs. For glassy polymers near room temperature, we observe values between 300 μs and 5–10 ms. The lowest value of $T_{CH}(ADRF)$ consistent with the experiments reported in section IIIG is about 50–100 ms, which is much too long to have a significant effect on the observed ^{13}C $T_{1\rho}$'s. Ordinarily, this is all the evidence one would need in order to decide whether or not spin–spin CP transfers were affecting $T_{1\rho}$. However, the ADRF experiments on polymers were only able to establish an approximate lower limit to the transfer rate. The experiment itself was not very satisfying since relatively short proton T_{1D}'s prohibited the determination of accurate transfer rates. We therefore feel that it is important to present additional evidence, which does not depend upon the ADRF experiment, and which is only consistent with the notion of the ^{13}C $T_{1\rho}$ for glassy polymers as a motional parameter.

(2) Theoretical predictions[30] of $T_{CH}(ADRF)$ (for $(H_1)_{carbon}$ = 30 G) are more than an order of magnitude longer than the longest observed ^{13}C $T_{1\rho}$. A typical $T_{CH}(SL)$ for a protonated methine carbon in an amorphous, glassy polymer with an ^{1}H line width of 5 G (20 kHz) is 50 μs. A value of $(H_1)_{carbon}$ = 30 G (30 kHz) is 50% greater than that of any rotating-frame dipolar field. This means, from the discussion surrounding Figure 6 of ref 30, that $T_{CH}(ADRF)$ can be expected to be between three and four orders of magnitude longer than $T_{CH}(SL)$, or about 100 ms. Such a prediction is consistent with the results of the ADRF experiments on polymers, but inconsistent with an important static CP effect (i.e., a CP effect in the absence of molecular motion) on the observed ^{13}C $T_{1\rho}$'s. Although the predicted numbers vary somewhat, this qualitative conclusion holds for all seven polymers of Table I.

(3) The observed ^{13}C $T_{1\rho}$'s are not a strong function of the applied $(H_1)_{carbon}$. In experiments on several polymers (including polystyrene) in which $(H_1)_{carbon}$ was varied by a factor of 1.5, we have observed relatively minor changes in the ^{13}C $T_{1\rho}$, consistent with an approximately square-law dependence. If the ^{13}C $T_{1\rho}$ were significantly influenced by static CP processes, however, we would, from theoretical and experimental analyses of the field dependence of $T_{CH}(ADRF)$, expect changes of at least an order of magnitude, consistent with a near exponential dependence.[30,32]

(4) Within the same polymer, carbon resonance lines which have the shorter $T_{1\rho}$'s can have the longer $T_{CH}(SL)$'s, while those with the longer $T_{1\rho}$'s can have the shorter $T_{CH}(SL)$'s.

The most prominent, but by no means the only, example of this phenomenon is poly(methyl methacrylate). The high-field α-methyl-carbon line has one of the shortest T_{CH}(SL)'s, while the quaternary-carbon line has one of the longest (Figure 3). Nevertheless, the quaternary-carbon line has a short $T_{1\rho}$ while the α-methyl-carbon line has one of the longest (Figure 5). This is totally inconsistent with the behavior expected[30] if the ^{13}C $T_{1\rho}$'s were dominated by static CP processes, in which case, on a relative basis, short T_{CH}(SL)'s would mean short T_{CH}(ADRF)'s and hence short $T_{1\rho}$'s.

(5) In comparisons between polymers, carbon resonance lines which have the longer $T_{1\rho}$'s can have the shorter T_{CH}(SL)'s and T_{CH}(ADRF)'s. Although the emphasis in this paper is on amorphous polymers, we have made measurements on polymers which are partially crystalline in nature, two examples of which are *isotactic* polystyrene and poly(phenylene sulfide) (Phillips Petroleum Co.). The latter polymer is a structural analogue of poly(phenylene oxide), based on a bridging sulfur linkage but missing the ring methyls. Both polymers have shorter proton T_2's, shorter protonated carbon T_{CH}(SL)'s, and longer ^{13}C $T_{1\rho}$'s than their glassy analogues. This result is inconsistent with a significant static CP effect on the short $T_{1\rho}$'s of the glassy polymers.

(6) For a given carbon of a polymer under magic-angle spinning conditions, the experimental $T_{1\rho}$ can show a dispersion of almost two orders of magnitude, while the $T_{1\rho}$ variation across an anisotropic chemical shift dispersion of a nonspinning polymer is about a factor of 2. The origin of the $T_{1\rho}$ dispersion will be discussed later in this section. For the moment, assume the dispersion arises from a geometrical orientation effect,[19] which could be its only origin if $T_{1\rho}$ were linked to, or dominated by, static CP processes, characterized by a T_{CH}, and determined exclusively by static dipolar interactions. If this were true, however, we would expect, in $T_{1\rho}$ experiments, large variations in the appearance of nonspinning spectra (whose chemical shift anisotropies are functions of orientation), as well as changes in the line widths of spinning spectra (as those carbons with orientations associated with dipolar interactions difficult to remove by decoupling are preferentially relaxed). None are observed (Figures 5, 8, and 13).

All of the evidence presented in the previous six paragraphs is only consistent with a description of the ^{13}C $T_{1\rho}$ as a rotating-frame motional parameter for glassy polymers near room temperature. Furthermore, all of this evidence involves undeniably large and unambiguous effects. There is an additional body of evidence, which we shall not enumerate here, involving smaller effects, arising from the many possible comparisons between polymers. Without exception, this evidence also supports the idea of the ^{13}C $T_{1\rho}$ as a motional, or what we will refer to as a spin–lattice parameter. We conclude, therefore, that for glassy polymers near room temperature the ^{13}C $T_{1\rho}$ is indeed a spin–lattice parameter. As such, it is sensitive to *rotational* segmental motions of the polymers in the frequency range specified by $(H_1)_{carbon}$, the applied rf field,[33] by the same physical arguments[11] that allow one to conclude that the spin–lattice parameter T_1 is sensitive to motions of the polymer in the frequency range specified by H_0, the applied static field.

Carbon-13 $T_{1\rho}$'s for glassy polymers are short, orders of magnitude shorter than T_1's. In fact, protonated carbon ^{13}C $T_{1\rho}$'s are often shorter than the proton $T_{1\rho}$ of the same polymer, especially for systems such as the poly(aryl ethers) which contain relatively few protons and have, therefore, relatively weak ^1H–^1H dipolar interactions. Since the $(H_1)_{carbon}$ rf fields used are greater than the local dipolar fields, the ^{13}C $T_{1\rho}$'s can be interpreted qualitatively in terms of Bloembergen–Pound–Purcell theory,[34] as applied to rare-spin rotating-frame NMR relaxation processes[32,33] without reference to the strong-collision theory of Slichter and Ailion.[35] That is, for ^{13}C spins quantized along an H_1 (greater than ^1H–^1H dipolar fluctuations), the *nonsecular* spin–lattice part of the I–S interaction ($I_zS_\pm$, using the notation of ref 32 with I = ^1H and S = ^{13}C) is not dominated by mutual ^1H–^1H spin flips, but rather by ^{13}C spin flips. These are induced by components of molecular motion near $(H_1)_{carbon}$. In the presence of even slow motion, a Debye component is generated at the rotating-frame Lamor frequency and so influences the ^{13}C $T_{1\rho}$ relaxation.

A second relaxation mechanism may exist. The modulation of ^1H–^1H dipolar fluctuations by motions can conceivably give rise to a stationary ^1H-^{13}C interaction corresponding to a substantial Hartmann–Hahn mismatch in frequency.[31] Thus, a contribution to the ^{13}C $T_{1\rho}$ is feasible from the *secular* part of the I–S interaction ($I_\pm S_\mp$). Since this contribution depends upon lattice motions within or spinning of the solid, we classify it as spin–lattice, although it involves a spin–spin transfer. In view of the results reported in paragraph (1) above, we suspect this contribution to $T_{1\rho}$ is small for glassy polymers near room temperature.

Approximate effective correlation times for the main-chain motions of glassy polymers can be obtained from ^1H $T_{1\rho}$ measurements.[7] The results of these experiments indicate that average correlation frequencies of the motions near room temperature are less than a typical ^{13}C $T_{1\rho}$ rotating-frame Larmor frequency of 30 kHz. This is consistent with our observation that main-chain carbon $T_{1\rho}$'s generally increase with increasing $(H_1)_{carbon}$ well below T_g, while the reverse is true for rubbers above T_g. Thus, in comparisons between polymers, the shorter $T_{1\rho}$ (measured at 30 kHz) indicates the greater average mobility. Complications in this kind of a simple interpretation of the ^{13}C $T_{1\rho}$ of glassy polymers may be encountered at low temperatures, where $T_{1\rho}$ has increased and T_{CH} decreased. Of course, minor complications are always produced by magic-angle spinning which introduces rotational motion which can itself be a source of spin–lattice relaxation.[36] (We will consider a specific example of the latter behavior, as well as the general problem of quantitative interpretation, in section VIB.)

(B) Some Properties of the ^{13}C $T_{1\rho}$ Dispersion. A prominent feature of the $T_{1\rho}$ plots of glassy polymers, such as those shown in Figure 10, is that they often are not linear. In general, this nonlinearity cannot be attributed exclusively to a fundamentally nonexponential relaxation process which occurs when the correlation time of the molecular motion generating the relaxation is comparable to the relaxation time itself.[37] We reach this conclusion on the basis of the fact that nonlinearities in $T_{1\rho}$ plots for the protonated and nonprotonated aromatic-carbon lines of poly(aryl ethers) are the same, even though protonated carbon $T_{1\rho}$'s are almost an order of magnitude shorter than nonprotonated values. Since both carbons necessarily share the same motions and are relaxed by the same protons, if a fundamentally nonexponential relaxation process were operating, we would expect the nonlinearity for the protonated carbon $T_{1\rho}$ plot to be more pronounced. It is not. Apparently, correlation times of 100 μs (5 kHz motion) are sufficiently shorter than typical 1000 μs $T_{1\rho}$'s that pronounced nonlinearity in the relaxation process itself does not occur (cf. section VIB). Thus, the NMR relaxation time can be thought of as resulting from a simplifying time average over the complexity of the molecular motions.

The nonlinearity in $T_{1\rho}$ plots can be interpreted as due to the presence of a multiplicity of relaxation times for otherwise sharp (under magic-angle spinning conditions) and well-defined lines. This is the sort of phenomenon which might be expected for mixed phase systems, in which the various component phases had significantly different motional properties, described by significantly different relaxation times, but had sufficiently similar chemical properties that

no net chemical shift differences were apparent.[23] The glassy polymers of Table I, however, are nominally homogeneous, single-phase systems (cf. section IIC). They are not high surface-area materials and contain no internal static domains of varying density which could be detected by any of a variety of scattering experiments. The origin of the nonlinearity is therefore not a static heterogeneity.

The ratio of fastest to slowest $T_{1\rho}$ relaxation rate implicit in non-linear plots such as those in Figure 10 is what we refer to as the dispersion in $T_{1\rho}$ relaxation times, or the $T_{1\rho}$ dispersion. The experimental $T_{1\rho}$ plots (including accurate initial slopes determined from expanded plots similar to those shown in Figure 11) are not well fit using a sum of only two $T_{1\rho}$'s, so the dispersions require the existence of at least three or, more likely, many relaxation rates.[38] Spin–lattice parameters describing relaxation in amorphous solids invariably show dispersions because of differences of the orientation of internuclear vectors connecting spin magnetic moments within the solid relative to the applied field, H_0.[19] However, these differences lead to rather small dispersions in the spin–lattice parameters, often difficult to detect, and, except for an occasional unusual singularity, not exceeding on the order of a factor of 2.[19] The observed differences between initial and final slopes of magic-angle ^{13}C $T_{1\rho}$ plots for the aromatic carbons of polymers such as polycarbonate and poly(phenylene oxide) can involve a factor of 50. Thus the origin of the $T_{1\rho}$ dispersion is not the usual amorphous solid orientation effect. Of course, the presence of strong intermolecular cross-relaxation between the protons of these polymers eliminates the possibility of a cross-correlation effect on the ^{13}C $T_{1\rho}$'s.

We now present the evidence supporting the conclusion that the ^{13}C $T_{1\rho}$ dispersion is not obscured by possible experimental artifacts but is, in fact, a useful and informative property of *molecular dynamics* influencing the ^{13}C spin system.

(1) The $T_{1\rho}$ dispersion is not significantly affected by the "spoil" sequence of Figure 1. The method of measuring the ^{13}C $T_{1\rho}$ is by a CP preparation of the carbon magnetization followed by a variable time held in $(H_1)_{carbon}$ with $(H_1)_{proton}$ turned off. A CP preparation is essential to avoid the artifacts[13] which would be generated by a single-resonance carbon spin-locking pulse. We feel that accounting for the $T_{1\rho}$ dispersion by a transient in the carbon magnetization resulting from the abrupt turn-off of $(H_1)_{proton}$ is unlikely since the nonlinear part of the $T_{1\rho}$ plot clearly persists for more than 1 ms (Figures 10 and 13), while the time constant for the turn-off is only 1 μs. (The latter time constant was measured by the response of the ^{1}H tuned circuit detected by a remote pick-up coil.) Furthermore, introducing repeated perturbations by ^{1}H 90° pulses, each separated by an ^{1}H T_2 (Figure 1), does not make the dispersion more pronounced and actually has no substantive effect on the $T_{1\rho}$ relaxation behavior in general. Finally, the carbon magnetizations observed for very short rotating-frame times without CP contact, times of 5–10 μs, are indistinguishable from those observed for the same experiment but without interruption in $(H_1)_{proton}$. We conclude that the dispersion is not an artifact resulting from transients in the ^{1}H channel transferred to the ^{13}C channel.

(2) The $T_{1\rho}$ dispersion is not pronounced for nonpolymeric materials. The average ^{13}C $T_{1\rho}$ we observe for adamantane, for example, is about 10 ms for an $(H_1)_{carbon}$ of 4 G, or 4 kHz at 22.6 MHz. (Note that this $T_{1\rho}$ is ten times longer than T_{CH}(SL) even though the ^{13}C H_1 is less than half of the proton room-temperature line width of 9 kHz; the ^{13}C $T_{1\rho}$ increases another factor of 20 when the $(H_1)_{carbon}$ is increased to 8 G, the latter still less than the adamantane ^{1}H line width.) Because there are no slow motions in the kHz range for adamantane, the observed relatively short ^{13}C $T_{1\rho}$'s are, in fact, the result of spin–spin CP transfers, which can be characterized by T_{CH}(ADRF)'s determined by the small $(H_1)_{carbon}$'s. Nevertheless, the dispersion associated with the adamantane $T_{1\rho}$ is less than a factor of 3. This is about what one would expect for effects in solid powders due to variations of orientations relative to H_0. It is far less than $T_{1\rho}$ dispersions often observed for glassy polymers. This is true despite the fact that in the adamantane experiment, ^{13}C–^{1}H spin–spin contact has been intentionally introduced. Consistent with the arguments of section VA, we conclude that the $T_{1\rho}$ dispersion in polymers does not result from transients in the ^{1}H spin system somehow transferred to the carbons by a spin–spin process.

(3) The $T_{1\rho}$ dispersion is not related to whether a particular carbon has a large chemical shift anisotropy or whether it is protonated or quaternary. The same $T_{1\rho}$ dispersions (ratio of fastest to slowest $T_{1\rho}$ relaxation rates) are observed for the aromatic- and methyl-carbon lines of poly(phenylene oxide), despite order of magnitude differences in chemical shift anisotropies; the same $T_{1\rho}$ dispersions, within experimental error, are observed for the protonated and nonprotonated carbon lines of poly(ether sulfone). The conclusion one can draw from these observations, particularly the latter observation, is that the dispersion is not related to variations in the ratio of $(H_1)_{carbon}$ to the undecoupled carbon line width, which might have been expected[39] to cause variations in $T_{1\rho}$'s, or to the operation of some nondipolar relaxation mechanism.

(4) The $T_{1\rho}$ dispersion can be different for lines arising from different carbons in the same polymer in the same experiment. There is only a small dispersion for the quaternary- and methyl-carbon lines of polycarbonate, while, under spinning conditions, there is a pronounced dispersion for the aromatic-carbon lines of that polymer. This observation, confirmed by repeated experiments, eliminates, for example, the possibility of variations in $T_{1\rho}$'s due to inhomogeneities in $(H_1)_{carbon}$.[39] (Homogeneous H_1's are to be expected in view of the truncated nature of the rotor sample which fits well inside the carbon rf coil.) Polystyrene provides another example of different dispersions for different carbons in the same polymer (both with and without spinning). There is only a minor $T_{1\rho}$ dispersion for the aromatic-carbon lines of polystyrene, with a more pronounced dispersion for the main-chain carbon lines.

(5) The $T_{1\rho}$ dispersion for some carbon lines is a function of the magic-angle spinning frequency. For example, the $T_{1\rho}$ dispersion for the protonated aromatic carbon line of polycarbonate is more pronounced under 3-kHz magic-angle spinning. (A molecular interpretation will be offered in section VIB.) This is not a general phenomenon, however, and is not observed for either the methyl-carbon line of polycarbonate or, for example, for any of the carbon lines of polystyrene. The effect cannot be explained in terms of variations in pressure within the solid polymer rotor, arising from radial acceleration during spinning. For our rotors, we calculate the maximum pressure on the rim is less than 0.1 kbar, which is insufficient to induce any plastic flow or distortion, and which is some one to two orders of magnitude less than the pressure required to produce significant effects on NMR relaxation parameters.[40] Nevertheless, the dependence on spinning suggests the ultimate source of the dispersion can be traced to a motional effect.

(C) The Molecular Origin of the ^{13}C $T_{1\rho}$ Dispersion. The origin of the ^{13}C $T_{1\rho}$ dispersion is the inherent dynamic heterogeneity of a polymer glass. Theoretical descriptions of the configurational statistics of a polymer chain employing the rotational isomeric-state model[41] invariably stress the fact that while the dominant steric interactions controlling the average dimensions of the chain are in one sense short range, involving pair-wise nearest (or next nearest) neighbor interactions, they are, in another sense, necessarily cooperative

since each member of any given pair engages in interactions with two neighbors. The pair-wise interactions lead to a non-Markoffian many-body problem.[42] The ultimate model of chain dynamics necessarily becomes that of an Ising-lattice description, with all the long-range cooperativity implicit in such a description.[42] This means that the local flexibility of a main-chain carbon in a nominally homogeneous solid glass well below its glass transition temperature will depend not only upon the configuration of the repeating units nearest to it in the chain but also, via connected pair-wise interactions, upon more distant units in the chain. The net result can be a pronounced heterogeneity in dynamic environments. Instead of local flexibilities and torsional motions dominated by the steric effects of the one or two highly preferred configurations or conformations of nearest neighbors, a given carbon in a main chain may be in any of a multiplicity of significantly different environments. Unlike the behavior observed for liquid or rubbery polymers,[8] frozen configurations and conformations in the glass are not rapidly interconverting, so there is no averaging of these environments. Thus, even though the torsional motions within the local configurations are cooperatively coupled, these motions can be different in different parts of the sample. It is just this heterogeneity which gives rise to the observed $T_{1\rho}$ dispersion.[38] At this point, we should caution that we consider unanswered the question as to the degree to which the $T_{1\rho}$ dispersion reflects motional cooperativity *beyond* the first few neighbors (in other words, the degree to which the $T_{1\rho}$ dispersion can be considered a truly long-range parameter).

Model calculations of cooperative motions in chain molecules[43] have been used in the past to interpret the dielectric loss spectra of solid polymers.[44] These calculations emphasize the dynamic heterogeneity of an Ising-type polymer system, which, in turn, successfully explains the width and asymmetry often observed in dielectric loss curves.[44] A crucial difference between the manifestation of dynamic heterogeneity in the dielectric loss experiment relative to that in the ^{13}C NMR experiment is that, in the former, an average power absorption over the entire sample is obtained. In the ^{13}C NMR experiment, on the other hand, the relaxation times[45] of individual components of the carbon magnetization from different parts of the sample are not averaged. This occurs because of the *magnetic* isolation of rare spins. As a result, different local configurations, which are not rapidly interconverting in the glassy state, lead to a multiplicity of ^{13}C relaxation times or the $T_{1\rho}$ dispersion.

In principle, each component of the experimental dispersion of relaxation times can be related to the appropriate distribution of correlation times associated with the cooperative microscopic motions responsible for the nuclear relaxation by means of well-established NMR theory.[34] Consequently, the ^{13}C NMR experiment contains more accessible information about the heterogeneity of local chain dynamics than dielectric or mechanical loss measurements. The latter experiments, because of their inherent averaging, superimpose the effects of cooperative motions with those of noninterconverting local configurations. Of course, ^{1}H NMR measurements totally suppress the distinction by averaging the NMR relaxation parameters through ^{1}H–^{1}H spin diffusion.[11,32]

So far, we have implicitly assumed that the dynamic heterogeneity characteristic of correlated motions in polymer main chains was predominantly intramolecular in origin and interpretable using the Ising-lattice configurational physics of single chains. (This theory invokes the cancellation between the chain-expanding influence of excluded volume effects and the chain-contracting influence of interchain effects, in order to be able to consider only isolated single chains in the solid.[46]) Although the origin of the $T_{1\rho}$ dispersion may be primarily intrachain in nature, there is experimental evidence which shows the dispersion cannot be *exclusively* intrachain in origin. For example, we know that the quenching of polycarbonate[16,47–49] freezes into the glass nonequilibrium, energetically unfavorable chain configurations.[50] In an exclusive intrachain description these states would be characterized by steep interactive potentials and so relatively high-frequency motion and short ^{13}C $T_{1\rho}$'s. These unfavorable states are removed as the glass slowly approaches its equilibrium state under the influence of prolonged annealing. As a result, for the new lower energy configurations, the intrachain potentials must be reduced in steepness. Thus, the frequency of the torsional oscillations within these potential wells would decrease. This expectation is, in fact, consistent with the experimental observation that the short $T_{1\rho}$'s characteristic of fast motion have been eliminated by annealing. However, while the frequency of motion for the annealed sample is, on the average, decreased in the absence of any other interactions, the intrachain description would require that the amplitude of the torsional oscillations within the flatter wells must be increased. We would therefore expect to see increased T_{CH}'s reflecting the removal of more static dipolar interactions by larger amplitude (even though lower frequency) motions. This is not observed.

It seems reasonable to us that the shapes of the interactive potential barriers depend, in fact, on interchain interactions. This dependence explains the restrictions on amplitudes of motion in the solid state. Interchain interactions are necessary not only to account for the results of the annealing experiment on T_{CH} but also for observations such as the absence of large-amplitude conformational jumps for the solid poly(aryl ethers) (cf. section VIC). We conclude therefore that a complete description of the dynamic heterogeneity of a polymer glass must include the effects of inter- as well as intrachain steric interactions. Presumably, both effects can be cooperative in the Ising-lattice sense and are correlated with one another.

This notion of both intra- and interchain cooperativity within a polymer glass is consistent with the results of other experiments sensitive to the effects of correlated motions. We have already discussed how *intra*chain cooperative motions have been cited to explain dielectric loss measurements in solid polymers.[43] The effect of *inter*chain correlations is apparent in light-scattering experiments.[51] The considerable disparity between optical anisotropies determined from depolarized light scattering for infinitely dilute solutions of chain molecules (in an isotropic solvent), relative to those for the undiluted polymer, is evidence of intermolecular correlations.[52] These correlations tend to be comparable in magnitude for both short alkanes and for long-chain polymers. This suggests a correlation range extending over segments of only three or four chains even in the solid. Although the light-scattering experiments do not demand that these correlations be explained in terms of a parallelization of neighboring chains,[52] such a conclusion helps to explain trends in chain packing in glassy polymers. Thus, amorphous vinyl polymer macroscopic densities tend to approach values observed for crystalline modifications of the same polymer only when the polymers contain bulky or polar side groups. These groups can be reasonably assumed to encourage parallelization thereby minimizing steric interactions.[53]

Naturally, this parallelization is not sufficient to enforce irregular, extended intrachain conformations. Thus, the configurational statistics of chains in the solid remains that of a random coil, consistent with neutron scattering determinations of end-to-end distances in glassy polymers.[54,55] That is, the parallelization of chains does not interrupt the predominant disorder within the glass. Nevertheless, the interchain correlations presumably influence the torsional

motions of the chain *within* given conformations and hence participate in generating the dynamic heterogeneity of the solid. By this interpretation, some of the more mobile chain segments (short relaxation time components of the $T_{1\rho}$ dispersion) can be assigned to the more disordered (little chain parallelization) regions of the glass. Thus, annealing homogenizes the glass by improving the local chain packing, increasing chain parallelization, decreasing the free volume, and decreasing the average segmental mobility (cf. the discussion of the bottom of Figure 22, near the end of section VID).

VI. Details of the Motions of the Polymers in the Solid State

In this section we will discuss the results of those ^{13}C NMR experiments which can lead directly to an understanding of some of the molecular details of motions of various polymers in the solid state.

(A) Poly(methyl methacrylate). The most unusual feature of the $T_{1\rho}$ experiment on poly(methyl methacrylate) (Figure 5) is the extraordinarily fast relaxation of the quaternary-carbon line, both with respect to the relaxation rates of some of the other carbons in poly(methyl methacrylate), as well as to the relaxation rates of nonprotonated carbons in other polymers (Figures 8 and 13). We attribute this fast relaxation as due to motion of the quaternary carbon relative to the four neighboring methylene protons. We suggest that this motion may be a 10-kHz, four-carbon, three-bond, main-chain crankshaft rotation, restricted to oscillations within fixed conformations. Presumably, the motion involves some torsional bond-angle distortion through greater rotation of the methylene carbon and its protons than of the quaternary carbon. This would account for the short quaternary-carbon $T_{1\rho}$ and the longer $T_{1\rho}$'s of the α-methyl and ester-methyl carbon lines, even though the latter carbons are protonated, and are connected to the quaternary carbon (and so share its motions). The assumption of some minor bond-angle distortion does not seem unreasonable to us, so long as the torsional motion involves angular excursions of only a few degrees. (Whether this torsional motion is simple classical rotation is not established; this particular NMR experiment contans no information about the mechanism of motion.) The main-chain torsional motion in poly(methyl methacrylate) is not a long-range motion, since the absence of a pronounced $T_{1\rho}$ dispersion indicates a lack of cooperativity (section VC). The motion cannot be coupled into large-scale side-chain motion since the nearly full chemical shift anisotropy[56] observed for the carboxyl carbon indicates that the overall motion of the side group must be quite restricted at room temperature. The latter result is consistent with mechanical and dielectric measurements from which it had been concluded that the frequency of the ester side-group motion at room temperature is of the order of 1 to 10 Hz.[57]

(B) Polycarbonate and Quantitative Interpretations of $T_{1\rho}$. The magic-angle ^{13}C NMR spectra of polycarbonate suffer from the unfortuitous overlap of the resonances arising from the carboxyl and nonprotonated aromatic carbons (Figure 6). Fortunately, however, the FT spectra of *non*-spinning polycarbonate are well enough resolved to be informative (Figure 7). Thus, the substantial Overhauser enhancement of the distinct low-field shoulder of the nonspinning spectrum leads directly to an assignment of a large NOE for the carboxyl carbon. This, in turn, means that the carboxyl carbon is involved in segmental motions, conceivably with some bond-angle distortion, in the MHz range.[8] The only other carbon in polycarbonate with a large NOE, and hence involved in high-frequency motions at room temperature, is, not surprisingly, the methyl carbon with its essentially unhindered internal rotation. Although the aromatic rings in the main chain are not engaged in high-frequency motions in the MHz range, we know from the $T_{1\rho}$ experiment (Figures 8 and 10) that these carbons are engaged in motions in the kilohertz range. We conclude that the carboxyl carbon in polycarbonate can be considered to act as a flexible link between aromatic rings in the main chain. We suspect two rings, bridged by the quaternary carbon, comprise the operating composite unit. As evidenced by pronounced $T_{1\rho}$ dispersions (cf. sections IIIB and VC), these units, linked by flexible carbonyl carbons, engage in correlated or cooperative motions in the kilohertz range. These motions must be in the low end of the kilohertz range, perhaps on the order of 10 kHz. This conclusion is based on the fact that the ^{13}C $T_{1\rho}$ dispersion for the protonated aromatic carbons is increased under magic-angle spinning conditions. This, in turn, is consistent with some main-chain aromatic groups undergoing relatively large mid-frequency excursions, a combination which produces moderately short relaxation times. Magic-angle spinning then modulates the spectral density associated with these motions (Figure 19) thereby increasing the density near the rotating-frame Larmor frequency and so producing some short $T_{1\rho}$ relaxation components.

In fact, for many of the polymers, spinning shortens both ^{13}C and ^{1}H $T_{1\rho}$'s slightly by modulating existing low-frequency motional components (weak modulation of strong static interactions is ineffective[31]) producing additional Debye spectral density near the rotating-frame Larmor frequency. In most situations, however, this is a small effect and only for polycarbonate and poly(phenylene oxide) are main-chain $T_{1\rho}$'s altered by as much as a factor of 2. (For the latter polymer, for example, the proton $T_{1\rho}$ is reduced from 30 to 20 ms by 3-kHz spinning, as measured by T_{CH} experiments similar to those illustrated in Figures 3 and 9.) Our use of the ^{13}C $T_{1\rho}$ in section VII will be as a semiquantitative measure of the presence of all types of main-chain motions in the low- to mid-kilohertz region, and for this purpose the complication introduced by the effect of spinning can be ignored.

Because of a variety of complicating factors, we have attempted no quantitative interpretation of the ^{13}C $T_{1\rho}$'s in terms of the motions in the solids. These complications include (1) the dynamic heterogeneity of the polymers themselves (section VB); (2) the fact that local dipolar fields, although smaller than $(H_1)_{carbon}$, are still comparable to it (section VA); (3) the effect of spinning on $T_{1\rho}$, mentioned above; (4) the contribution to the $T_{1\rho}$ dispersion due to differences of static orientations relative to the applied magnetic field, H_0; (5) the possibility of some nonlinearity in $T_{1\rho}$ behavior due to the presence of a few slow motions with correlation times comparable to $T_{1\rho}$ (section VB); and, finally, (6) the possibility of contributions (consistent with the arguments of section VA) to ^{13}C $T_{1\rho}$'s from ^{1}H–^{1}H dipolar fluctuations modulating dynamic ^{1}H–^{13}C interactions.[5,30,31] While none of these complications change the *qualitative* notion of the ^{13}C $T_{1\rho}$ as an indicator of motion, they do make difficult a rigorous quantitative specification of the amplitudes, frequencies, and correlation times describing the slow motions of the polymers.

(C) Poly(phenylene oxide). The magic-angle CP ^{13}C NMR spectra of poly(phenylene oxide) are actually more detailed than the corresponding FT spectra of the polymer in solution. An unexpected feature of these spectra (Figure 12) is that the second line from the right (which can be unambiguously assigned to the protonated carbons of the aromatic rings) is a singlet in solution and a doublet in the solid state. Inspection of models of the chain (Figure 21) shows that the two protonated carbons of the ring need not be equivalent because of the nonlinearity of the C–O–C bond. These two carbons become equivalent in the event of free rotation about the O–C bond. This apparently occurs in solution but does not occur in the solid state. The relaxation behavior of the doublet

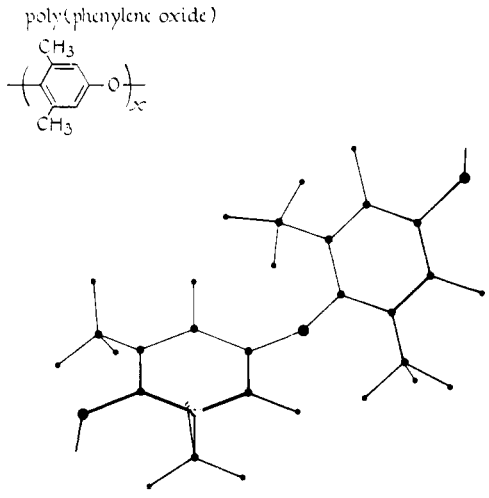

Figure 21. A spatial representation of two units in a poly(phenylene oxide) chain.

proves that in the solid state *all* the aromatic rings of amorphous poly(phenylene oxide) are restricted to torsional oscillations about an asymmetric equilibrium orientation. Fine structure, similar to the doublet, is also hinted at in the spectra of some of the other glassy polymers, poly(ether sulfone) in particular. In fact, unresolved fine structure, arising from asymmetric chain configurations, may also explain why the methyl-carbon resonances of polycarbonate and polysulfone are consistently broader than the quaternary- and protonated aromatic-carbon resonances of those two polymers. The presence of resolved or partially resolved fine structure in the solid-state spectra of the poly(aryl ethers) show that, for these polymers, main-chain torsional motions necessarily cannot involve large-amplitude conformational jumps, since such jumps would, of course, average out any fine structure.[38]

While the absence of free rotation in the solid might seem reasonable on intuitive grounds, calculations[58] of the barrier to rotation in poly(phenylene oxide) predict virtually free rotation. Furthermore, on the basis of such calculations, the mechanical impact strength of poly(phenylene oxide) has been, in the past, interpreted in terms of the ability of an inherently flexible chain to dissipate energy internally.[58] Our ^{13}C results, of course, are *only* consistent with the absence of free rotation. Thus, we can eliminate a mechanism for toughness in poly(phenylene oxide) based on the ability of the polymer to undergo rapid *reversible* transformations between conformations separated by large angular displacements. We will discuss in section VII an alternate explanation of toughness in polymers.

A second type of magic-angle spectrum of poly(phenylene oxide) is shown in Figure 14. In these experiments short CP contact times were used to generate what can be described as a "magic-angle hole". Cross-polarization transfer from protons to carbons is inefficient for those particular internuclear ^{13}C–^{1}H vectors in the amorphous nonspinning solid which happen to have an orientation relative to H_0 of 54.7°.[4] Carbons in this situation can be distinguished from other carbons by their chemical shift, which also is a function of orientation relative to H_0, when the chemical shift tensor has the form of a symmetric top with the unique axis lying along the effective ^{13}C–^{1}H internuclear vector. For short contact times a hole appears in the spectrum as carbons whose ^{13}C–^{1}H vectors are at the magic angle are not polarized. The methyl-carbon chemical shift anisotropy is sufficiently well defined for poly(phenylene oxide) that this hole is obvious. The hole will not be blurred by restricted high-frequency motions (where high frequency now means frequencies much greater than the chemical shift dispersion). This occurs because the high-frequency motion (including internal rotation) may alter the pattern of the chemical shift anisotropy but still leaves average ^{13}C–^{1}H vectors with residual static orientations of 54.7° relative to H_0. Slow motions, on the other hand, will tend to blur or obscure the hole because a well-defined magic angle does not exist during the experiment. The latter appears to be the situation for polycarbonate (Figure 14), where the hole is barely visible despite the fact that the methyl-carbon chemical shift anisotropy is clear. We can conclude therefore that main-chain motions in the 100-Hz range are less common for poly(phenylene oxide) than for polycarbonate, at room temperature.

The $T_{1\rho}$ dispersions of poly(phenylene oxide) are all the same, which is reasonable since the slow motions of all the carbons are tied together by the rigid phenyl ring. This is in contrast to systems such as polycarbonate where the absence of a pronounced effect of spinning on methyl- and quaternary-carbon $T_{1\rho}$ dispersions shows that the bridging quaternary carbon is not included in all types of main-chain motions.

(D) Poly(vinyl chloride), Polystyrene, and Spectral Density Plots. The magic-angle ^{13}C NMR spectra of poly(vinyl chloride) and polystyrene are not sufficiently detailed that the methylene- and methine-carbon lines are resolved from one another. Nevertheless, ^{13}C $T_{1\rho}$ experiments show that the main-chain lines for both polymers are characterized by small dispersions, much less than those observed for individual lines of polycarbonate, polysulfone, and poly(phenylene oxide), as discussed in section V. Thus, unlike the situation for the polyaryl ethers, there is little evidence for strong, long-range cooperative main-chain motions in the vinyl polymers investigated to date. For these vinyl polymers, descriptions of motions which avoid specifications of molecular details, descriptions such as the "local-modes" theory of motion in polymer glasses,[59] may be perfectly adequate. That is, since little long-range cooperativity seems to be present for those significant main-chain segmental motions responsible for the NMR relaxation parameters, there is little point to specifying the influence of distant steric interactions by anything other than some sort of a statistical average.

The $T_{1\rho}$'s for main-chain carbon lines of poly(vinyl chloride) and polystyrene are comparable to those observed for the polyaryl ethers, while both the T_{CH}'s and T_1's are shorter.[1] Considering the frequency regimes important to each of these relaxation parameters,[4,8] these results suggest that a qualitative representation of relative spectral densities[28] describing segmental main-chain motions of comparable amplitude for the two classes of polymers would look something like that illustrated at the top of Figure 22.

The spectral density for vinyl polymers has considerably greater values at very low frequencies and very high frequencies, with somewhat less density in the mid-frequency range than the spectral density for the poly(aryl ethers). The areas under both distributions are, of course, equal. Flexible main-chain links in polycarbonate and polysulfone, directly bonded to bulky main-chain aromatic groups, probably produce large composite units well suited to long-range cooperative motions in the low- to mid-kilohertz frequency range at room temperature. We suspect that the vinyl polymers have increased density at high frequency (at room temperature) because the operational motion unit can involve only a few carbons in the main chain. The vinyl polymers are weak in mid-frequency range motions only in the sense that the absence of sterically free ether-type linkages blocks cooperativity along the chain. For polymers such as polystyrene, short-range, mid-frequency motions do occur, but their amplitudes are sufficiently small, and their cooperativity sufficiently limited, that they do not destroy the inherent rigidity of the

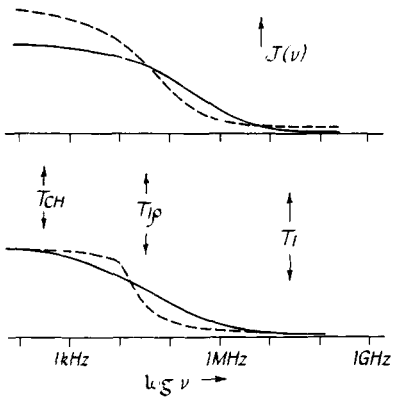

Figure 22. Schematic representation of spectral density associated with the main-chain motions of typical poly(aryl ethers) (top, solid), typical vinyl polymers (top, dotted), quenched polycarbonate (bottom, solid), and annealed polycarbonate (bottom, dotted).

chain. This main-chain rigidity also accounts for the observed short T_{CH}'s of the vinyl polymers. Note that it is not contradictory to think of a basically rigid vinyl polymer chain which is still capable of segmental motions in the kilohertz or megahertz range, when it is remembered that these motions involve torsional oscillations of only on the order of a few degrees.

The bottom of Figure 22 portrays, in a qualitative way, through the use of spectral density plots, our feeling as to what might be happening in annealing experiments, such as the annealing of polycarbonate discussed in section VC. Annealing removes energetically unfavorable intrachain configurations. The improbable intrachain configurations are generally those resulting in interchain environments permitting relatively more mobile main-chain carbons which can be detected in the $T_{1\rho}$ experiment. The removal of these configurations is communicated between and along chains through cooperative pairwise steric interactions. In short, the annealing produces a loss of free volume and a substantial redistribution of the spectral density describing the motions of a given chain, although that chain's average static configuration within the solid may be only slightly affected. Since only the mid-frequency range of motions is experimentally observed to be significantly altered, we represent the redistribution as shown, with the values of the spectral density at the extremes almost unchanged. As discussed earlier, annealing has reduced some of the dynamic heterogeneity of the glass. This is shown in Figure 22 (bottom, dotted) as a reduction of the broadness, or dispersion, of the spectral density associated with the motions of the annealed glass. Obviously, additional experiments are desirable to provide a more detailed and informative map of this redistribution. Nevertheless, the sharpening of the spectral density plot for annealed polycarbonate suggests that the observed mechanical embrittlement may be associated with a loss of the ability of the polymer to respond to a broad range of the mid-kilohertz Fourier components of an impact. This link between relaxation phenomena and mechanical properties will be discussed at length in the next section.

The presence of mid-frequency range motions for glassy polymers has some implications for the ultimate resolution possible in magic-angle spinning experiments. Some aspects of this problem have been discussed earlier in section IVA. Segmental motion in the 10^5-Hz range is anathema to combination dipolar decoupling-spinning experiments.[28] For example, if 10% residual dipolar broadening survived the resonant dipolar decoupling of an intermediate-frequency motion, which was restricted to 5% of all possible orientations, and if the full rigid-lattice dipolar line width possible were 10^4 Hz, then a residual dipolar line width of 50 Hz would be observed. This assumes the static dipolar component of the interaction could be totally removed by dipolar decoupling. A 50-Hz resolution is close to what we are presently achieving in our combination dipolar decoupling and magic-angle spinning experiments. For those polymers, with substantial mid-frequency segmental motions, a 50-Hz resolution may, in fact, be close to a lower limit, at least at room temperature.

VII. Carbon-13 Relaxation Parameters and the Impact Strengths of Glassy Polymers.

The importance of low-frequency main-chain motions in polymeric glasses has long been cited as a key to the understanding of mechanical properties such as toughness or impact strength.[60] For the last 25 years, these motions had been detected primarily by mechanical spectroscopy in which the mechanical or dielectric loss of a polymer was measured as a function of temperature between 100 and 300 K.[9] Low-temperature loss peaks ($T < T_g$) were hopefully identified with specific types of motions by a process of inductive and deductive reasoning. Behavior of the polymer at room temperature was then deduced by means of a temperature-frequency superposition principle. Correlations between the presence of low-temperature mechanical loss peaks and impact strength could be, in fact, established. Thus, it became clear that glassy polymers having no substantial low-temperature mechanical loss peaks (or no general background lossiness) were invariably brittle materials with low impact strength.[60]

Nevertheless, these correlations were, and are, not completely satisfying. Complications arise from at least two sources. First, there is no reliable way to establish the origin of a low-temperature loss peak. Thus, it became clear that loss peaks associated exclusively with either side-chain motions, or with absorbed water or residual monomer, or even with thermally induced changes between nonequilibrium conformational populations are not related to impact strength.[61] Uunambiguous identifications of individual low-temperature loss peaks with these processes have been rare however, and are, in most situations, not possible. As a result, semiquantitative predictions of impact strengths based on anelastic spectra (either using loss peaks or using total areas under the mechanical loss curve, integrated over a specified temperature range) are confused by the inability of separating from a peak or an integrated area, presumably monitoring main-chain motions, various irrelevant contributions.

The second source of complications affecting correlations between mechanical loss peaks and impact strength is the ambiguity inherent in the temperature-frequency superposition principle.[62] This principle assumes that only the frequency of a motion changes with temperature, and not the character of the motion itself. That is, if it is true that at low temperature a particular mechanical loss peak is associated with a side-group motion and does not involve main-chain motions, then it is assumed that at room temperature only the frequency of this motion has changed and not its character as a side-group motion. This requires that the activation energy of the motional process is independent of temperature,[63] which may or may not be true, depending on the temperature interval. As a result, predictions, based on mechanical loss data obtained at low temperature, of the presence or absence of motions important to impact strength at room temperature may be seriously in error. Of course, dielectric loss spectra obtained as a function of frequency at fixed temperature avoid a temperature extrapolation but generally are so broad and featureless[64] that an incisive analysis is impossible.

We propose that the use of ^{13}C NMR relaxation parameters characterizing molecular motions in polymer glasses can lead to simple, predictive descriptions of mechanical properties

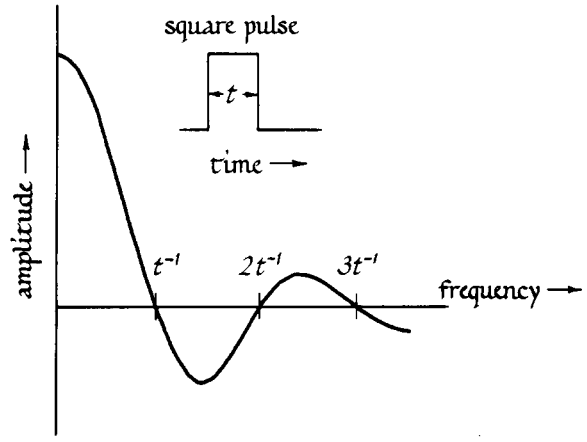

Figure 23. Spectral analysis of a finite pulse showing that the important frequency components of the pulse are of the order of the inverse of the pulse width.

such as impact strength, which are free from the ambiguities mentioned above. The basis for this proposal has been established in sections V and VI. In brief, the ^{13}C NMR experiments clearly identify the molecular origin of main-chain motions and characterize them with a variety of relaxation times, measured at room temperature, but covering different frequency ranges. From these relaxation times, a spectral density plot is constructed which describes the main-chain motions of the polymer *at a single temperature.* The relative values of spectral density for frequencies associated with the mechanical perturbations generated by an impact are, we claim, related to the inherent toughness of the polymer. In the remainder of this section we will present the analysis establishing the correlation between ^{13}C relaxation parameters and the impact strength of glassy polymers.

(A) Spectral Analysis of the Impact. A mechanical impact is an energy pulse of finite duration. A Fourier or spectral analysis[21] of such a pulse (Figure 23) shows that frequencies of the order of the inverse of the pulse width are important. High-speed mechanical testing has established that typical impact events have durations of about 100 μs.[65-68] (Ultra-high-speed collisions, arising, for example, from the impact of high-velocity bullets, have even shorter durations. We will not consider these processes in the following discussion.) Naturally, mechanical impacts are not idealized square or, more properly, rectangular pulses but can be expected to have some structure within their 100 μs duration. This structure will tend to obscure the local maxima and minima of plots such as Figure 23. Such structure will also generate higher-frequency components in the impact. It seems likely that the upper limit on frequency components necessary to describe an average high-speed mechanical impact is between 10 and 100 kHz. Since the total energy represented by the impact is less than the energy required to cause a polymer sample to fail in a slow stress–strain experiment,[69] it is clear that the inability of a polymer to cope with the kilohertz-range components of the impact is crucial to an understanding of toughness.

The mechanical behavior of a nominally uniform, void free, polymeric solid under impact can be described by a comparison of the spectral density of the main-chain motions of the polymer relative to the spectral density of the impact itself. For rigid polymers, with relatively few motions in the mid-kilohertz range, the spectral density is mismatched with that of the impact at both low and mid frequency (Figure 24, top). The mismatch in the mid-frequency range is critical since it reflects the inability of the solid to respond quickly to the impact. This inability leads to local stress concentrations, which, in turn, lead ultimately to crack formation and failure. For polymers with more flexible main chains, associated with spectral density distributions more closely matched to that of the impact (Figure 24, middle), more modes of long-range, cooperative main-chain motions are stimulated by the impact. This process avoids local stress concentrations by dissipation of energy through internal heating. The heating is directly related to the damping, or lossiness, of each of the various excited modes. For highly flexible chains (essentially rubbers above T_g), many components of the frequency distribution of main-chain motions are greater than even the highest of those of the impact (Figure 24, bottom). Even though the rate of energy dissipation of the impact is not as great as in the better matched case (Figure 24, middle), rapid failures of rubbers do not occur since the fracture-producing high-frequency components of the test are weak relative to the high-frequency components of motion of the polymer. Failures of rubbery polymers are related to the near static components of the test, which can produce excessive strains or elongations but only over relatively long periods of time.

Within the linear response region, the ability of the solid to cope with the energy of the impact is measured by the power absorption. This power absorption, in turn, is given by the Fourier transform of the autocorrelation function describing the chain motion.[70] We entertain no hope of calculating this autocorrelation function or of specifying any details of the chain motion as a stochastic process. Fortunately, we are not required to do so. The same autocorrelation function which leads to a measure of the power absorption (associated with the linear response to a given frequency component of the impact) also specifies the spectral density and ultimately ^{13}C NMR relaxation rates associated with motional processes occurring at this frequency.[71] Thus, if we wish to obtain a notion of the capacity for mechanical power absorption of a polymer near 10 kHz, for example, relative to that near zero frequency, we can do this by a ratio of suitable main-chain ^{13}C NMR relaxation rates sensitive to the two frequencies, such as, for example, $\langle T_{1\rho}\rangle^{-1}/\langle T_{CH}{}^{\dagger}\rangle^{-1}$. (The dagger indicates that for purpose of comparisons, T_{CH} has been reduced by removing, approximately, the dependence[5] of T_{CH} on the ^1H–^1H dipolar interaction, which varies somewhat from polymer to polymer.[11] [See footnote *b*, Table I.] This procedure is unnecessary for $T_{1\rho}$ which has no strong dependence on the ^1H–^1H interaction.)

(B) The Correlation. We suggest that the ratio $\langle T_{CH}{}^{\dagger}\rangle/\langle T_{1\rho}\rangle$ should correlate in a simple way with the impact strength of glassy polymers. The ratio can be thought of as a measure of the number of chain segments of a dynamically heterogeneous polymeric solid capable of dissipating the energy of an impact relative to the number of more rigid segments unable to respond to the impact. In particular, a short $\langle T_{CH}{}^{\dagger}\rangle$ is a measure of those chains, or chain segments, suited to coping with the near static components of the impact, but only capable of leading to stress concentrations when dealing with any higher frequency components. As mentioned earlier, these kilohertz-range components of the impact are responsible for the ultimate failure of the material. The correlation uses $\langle T_{CH}{}^{\dagger}\rangle$ in the numerator of the ratio so that a short $\langle T_{CH}{}^{\dagger}\rangle$ will lead to a small ratio, corresponding to a low impact strength. Similarly, a short main-chain $\langle T_{1\rho}\rangle$ (observed at, say, 30 kHz) measures chain segments inherently capable of dissipating impact energy as heat within the sample. Thus, a small value of $\langle T_{1\rho}\rangle$ in the denominator of the ratio will lead to a large number, corresponding to a high impact strength. Very fast motions of the chain are, as a first approximation, ignored in formulating the correlation, since they neither dissipate any of the energy of the impact nor lead to stress concentrations within the sample. Note that even though the NMR measurements may be performed using a ^{13}C rotat-

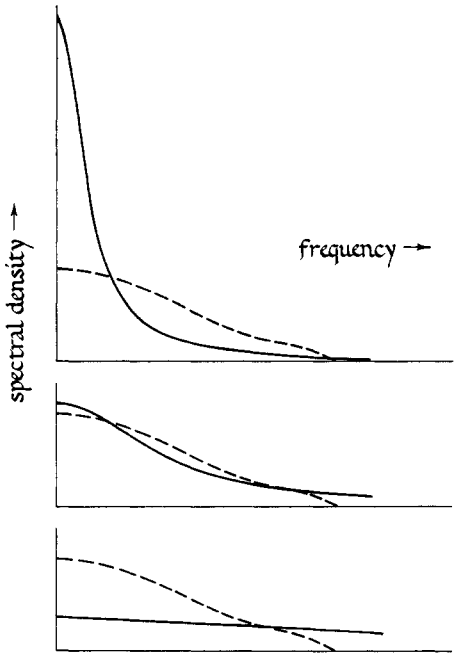

Figure 24. Comparison of the spectral density of a mechanical impact with that of the main-chain motions of a rigid glassy polymer (top), a more flexible glassy polymer (middle), and a rubber above T_g bottom). The spectral density of the mechanical impact is shown as the dotted curve in each case.

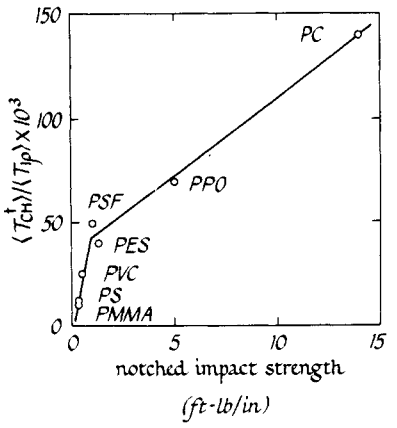

Figure 25. The correlation between notched impact strength, in ft lb/(in. of notch radius), and a ratio of ^{13}C NMR relaxation parameters. The abbreviations are polycarbonate, PC; poly(phenylene oxide), PPO; polysulfone, PSF: poly(ether sulfone), PES; poly(vinyl chloride), PVC; polystyrene, PS; poly(methyl methacrylate), PMMA.

ing-frame frequency near 30 kHz, a ratio of $\langle T_{CH}^{\dagger}\rangle$ to $\langle T_{1\rho}\rangle$ is not insensitive to chain motions at other frequencies in the low- to mid-kilohertz range. That is, motion at 10 kHz, for example, will contribute to shortening a $T_{1\rho}$ measured at 30 kHz. Actually, the ratio should be thought of as an attempt to describe the general shape of spectral density plots such as those shown in Figure 24, rather than as a definition of the density for two arbitrary frequencies.

A correlation of NMR relaxation parameters, measured on polymers under unstressed conditions, with impact strength would seem to have little chance to succeed.[72] A large part of the impact strength of a glassy polymer arises from energy dissipation during nonlinear plastic flow and crazing[73,74] and other stress-dependent cooperative or correlated processes.

Nevertheless, we feel the $\langle T_{CH}^{\dagger}\rangle/\langle T_{1\rho}\rangle$ ratio can be used to characterize events in this nonlinear regime. In particular, this is true of $\langle T_{1\rho}\rangle$. We have established in section VC that $T_{1\rho}$ is sensitive (through its dispersion which determines its average) to cooperative inter- and intramolecular motions of the polymer main chains. Plastic flow occurs in the sample following stress concentrations resulting from the inability of the polymer to dissipate elastically all the energy associated with the higher frequency components of the impact. While the flow may occur in times on the order of a millisecond, the initial cooperative slippage of chains must be a higher frequency process to cope with the rate[68] of stress concentration. The specific range of frequencies important to such stress-activated processes has not been established. However, we feel that the motions of chain segments whose main-chain carbons are characterized by a distribution of short $T_{1\rho}$'s (and relatively long $T_{CH}^{\dagger}$'s) are correlated well enough with the motions of neighboring segments *throughout* the low- to mid-kilohertz frequency range, that these motions can initiate the cooperative, nonlinear plastic flow which helps to dissipate the energy of intense impacts. For chain segments with short $T_{1\rho}$'s, but also short $T_{CH}^{\dagger}$'s, we feel the mid-frequency range motions are not sufficiently well correlated with those of their neighbors to permit relatively large amplitude motions (which would have averaged static dipolar interactions and produced long T_{CH}'s). Hence, these uncorrelated motions do not lead to cooperative flow under impact. In short, we suggest the $\langle T_{1\rho}\rangle$ to $\langle T_{CH}^{\dagger}\rangle$ ratio acts as a measure of the ability of the main-chain motion to trigger wide-scale, irreversible plastic flow.

We present the correlation in Table I and Figure 25.[75] Regardless of whether one subscribes to all the rationalizations of the previous paragraphs, it is clear a valid correlation exists between $\langle T_{CH}^{\dagger}\rangle/\langle T_{1\rho}\rangle$ and the impact strength for the seven glassy polymers investigated. Polymers having large ratios have high impact strengths, while those with low ratios have low impact strengths. (We do not place any particular significance on differences in ratios less than about a factor of 2 or so.) We emphasize that we have established here a correlation between the impact strength and a ratio of relaxation parameters, not a functional dependence.

(C) Limitations of the Correlation. The correlation between impact strength and ^{13}C relaxation parameters shown in Figure 25 is not expected to extend to events occurring in times much longer than a millisecond. That is, we see no reason to expect $\langle T_{1\rho}\rangle$ to contain information related to macroscopic crack propagation and its inhibition or accentuation by unusual boundary conditions or by second phases.[76] Thus, we do not expect successful simple correlations between NMR parameters and impact measurements made on rubber or particulate reinforced glasses, or on internally flawed or surface etched materials. Such systems are subject to static heterogeneities and stress fields, which are generated during fabrication by the macroscopic geometry of the sample. These heterogeneities can influence impact strength but are generally unrelated to microscopic chain dynamics. On the other hand, the NMR measurements are usually performed on thicker samples than those used in mechanical impact tests. While the NMR measurements are not affected by many static heterogeneities, they can be influenced by variations in orientation and free volume sometimes found in thick samples as a result of differences in cooling rates for different parts of the sample on passing through T_g. This ambiguity in the use of different physical samples limits to a qualitative nature the correlation between NMR measurements and mechanical properties.

The correlation incorporates no dependence on molecular weight. It is highly probable that the ^{13}C NMR measurements are not strong functions of molecular weight. Thus, the NMR parameters contain information about what might be called an idealized or inherent toughness of the polymer, which, if

the molecular weight is sufficiently high, should be, in fact, indicative of the impact strength. If the molecular weight is not high, the polymer glass is likely to be subject to one or more limitations, similar to those mentioned above, and so be outside the applicability of our correlation.

In addition to the above limitations, we note that the ratio of relaxation parameters selected for the correlation, while reasonable, is not the only, or even the best, way in which to correlate relaxation parameters and impact strength. After all, we are attempting to describe a complicated event, the response of a cooperative polymeric solid to an impact with the ratio of two numbers characterizing a representative main-chain carbon. Clearly, we would get improved results if we had used more accurate descriptions of the spectral density for these polymers than those afforded by just two values. That is, it would be desirable to have $T_{1\rho}$ at several frequencies for all main-chain carbons, so that we could, perhaps, use some sort of weighted average over the 5–100-kHz range. Furthermore, the ^{13}C undecoupled line width (T_2) would be a useful parameter to characterize static interactions. Although the protonated carbon T_2 is difficult to measure, the experiment is technically feasible.[77] Dispersions in T_2 plots would be far more apparent than in the corresponding CP transfer–rate plots, and such dispersions would contain valuable information about the possible heterogeneity of near static interactions.

Finally, it would be desirable to test the correlation of ^{13}C NMR parameters with impact strength at a variety of temperatures in order to confirm its generality. In particular, the embrittlement of some glassy polymers at low temperature is well known,[60] and the characterization of main-chain dynamics in this situation should be revealing (assuming no complications in the NMR experiment itself, cf. the end of section VA). The toughening of some brittle polymers at elevated temperatures should also be reflected in changing main-chain dynamics and ^{13}C $T_{1\rho}$'s. However, it is conceivable that at high temperatures some of the more flexible chains of a dynamically heterogeneous polymer glass will have $T_{1\rho}$'s on the high-temperature side of the $T_{1\rho}$ minimum. Thus, a simple connection between decreasing $T_{1\rho}$ and increasing segmental mobility would no longer be true. This would mean that while an impact strength–NMR relaxation correlation may remain generally valid, the numerical values would depend on the choice of rf field strength; that is, the correlation would depend on the choice of rotating frame Larmor frequency.

VIII. Summary

One-hundred hertz resolution has been achieved in the ^{13}C NMR spectra of solid polymers by a combination of resonant dipolar decoupling and magic-angle spinning. This spinning is totally compatible with cross-polarization procedures thereby producing a high-sensitivity, as well as a high-resolution, experiment. The high resolution permits individual resonance lines to be assigned to specific carbons in the polymer. This means that the interpretation of rare-spin NMR relaxation experiments in terms of the motions of the side and main chains of the polymers can be made unambiguously. For the first time, many aspects of motions in solid polymers can be identified and characterized without recourse to models and extrapolations, or appeals to intuition. In this regard, the ^{13}C $T_{1\rho}$ relaxation parameter is particularly informative since it is directly related to those motions of glassy polymer main chains which are in the low- to mid-kilohertz frequency range and which are vital in determining mechanical properties such as toughness.

Acknowledgments. We are pleased to acknowledge the helpful criticism and suggestions of T. R. Steger, R. J. Morgan, R. F. Boyer, and J. M. Deutch (regarding the nature of glassy polymers) and of D. L. VanderHart, J. S. Waugh, and K. J. Packer (regarding the interpretation of the CP ^{13}C NMR experiments).

References and Notes

(1) J. Schaefer, E. O. Stejskal, and R. Buchdahl, *Macromolecules*, **8**, 291 (1975); J. Schaefer and E. O. Stejskal, *J. Am. Chem. Soc.*, **98**, 1031 (1976).
(2) E. R. Andrew, *Prog. Nucl. Magn. Reson. Spectrosc.*, **8**, 1 (1971).
(3) S. R. Hartmann and E. L. Hahn, *Phys. Rev.*, **128**, 2042 (1962).
(4) A. Pines, M. G. Gibby, and J. S. Waugh, *J. Chem. Phys.*, **59**, 569 (1973).
(5) D. A. McArthur, E. L. Hahn, and R. E. Walstadt, *Phys. Rev.*, **188**, 609 (1969).
(6) We refer to the NMR spectra obtained in this way as "CP ^{13}C NMR spectra", or occasionally as "CP spectra". This is simply a convenient short-hand description, analogous to the familiar "FT NMR spectra", and should not be confused with the older use of the term "CP spectra" to describe plots of T_{CH}^{-1} as a function of the frequency mismatch of the Hartmann–Hahn condition.
(7) D. W. McCall and D. R. Falcone, *Trans. Faraday Soc.*, **66**, 262 (1970).
(8) See, for example, J. Schaefer, *Top. Carbon-13 NMR Spectrosc.*, **1**, 149 (1974).
(9) N. G. McCrum, B. E. Read, and G. Williams, "Anelastic and Dielectric Effects in Polymeric Solids", Wiley, New York, N.Y., 1967.
(10) T. M. Connor, "NMR, Basic Principles and Progress", Vol. 4, P. Diehl, E. Fluck, and R. Kosfeld, Ed., Springer-Verlag, New York, N.Y., 1971.
(11) D. W. McCall, *Acc. Chem. Res.*, **4**, 223 (1971).
(12) E. O. Stejskal and J. Schaefer, *J. Magn. Reson.*, **14**, 160 (1974).
(13) E. O. Stejskal and J. Schaefer, *J. Magn. Reson.*, **18**, 560 (1975).
(14) A. Pines and T. W. Shattuck, *J. Chem. Phys.*, **61**, 1255 (1974).
(15) W. Wrasidlo, *J. Polym. Sci., Part A-2*, **10**, 1719 (1972).
(16) S. E. B. Petrie, "Polymeric Materials", American Society of Metals, Metals Park, Ohio, 1975, p 55.
(17) E. O. Stejskal, J. Schaefer, J. M. S. Henis, and M. K. Tripodi, *J. Chem. Phys.*, **61**, 2352 (1974).
(18) L. F. Johnson, F. Heatley, and F. A. Bovey, *Macromolecules*, **3**, 175 (1970).
(19) M. G. Gibby, A. Pines, and J. S. Waugh, *Chem. Phys. Lett.*, **16**, 296 (1972).
(20) R. K. Hester, J. L. Ackerman, V. R. Cross, and J. S. Waugh, *Phys. Rev. Lett.*, **34**, 993 (1975).
(21) T. C. Farrar and E. D. Becker, "Pulse and Fourier Transform NMR", Academic Press, New York, N.Y., 1971, p 20.
(22) J. Schaefer, *Macromolecules*, **6**, 882 (1973).
(23) K. J. Packer, *Prog. Nucl. Magn. Reson. Spectrosc.*, **2**, 87 (1967).
(24) E. R. Andrew, W. S. Hinshaw, and R. S. Tiffen, *J. Magn. Reson.* **15**, 191 (1974).
(25) See, for example, G. C. Levy and G. L. Nelson, "Carbon-13 Nuclear Magnetic Resonance for Organic Chemists", Wiley, New York, N.Y., 1976.
(26) C. J. Carmin, A. R. Tapley, Jr., and J. H. Goldstein, *Macromolecules*, **4**, 445 (1971).
(27) N. Bloembergen and T. J. Rowland, *Acta Metall.*, **1**, 731 (1953).
(28) U. Haeberlen and J. S. Waugh, *Phys. Rev.*, **175**, 453 (1968).
(29) W. P. Slichter, *Rubber Chem. Technol.*, **34**, 1574 (1961).
(30) D. E. Demco, J. Tagenfeldt, and J. S. Waugh, *Phys. Rev. B.*, **11**, 4133 (1975).
(31) E. O. Stejskal, J. Schaefer, and J. S. Waugh, *J. Magn. Reson.*, in review.
(32) A. Abragam, "Principles of Nuclear Magnetism", Oxford University Press, London, 1961, p 565.
(33) Since the exponential dipolar relaxation is *heteronuclear*, the important frequency is the Larmor frequency, not twice the Larmor frequency. See, for example, J. H. STRANGE AND R. E. Morgan, *J. Phys. C.*, **3**, 1999 (1970).
(34) N. Bloembergen, E. M. Purcell, and R. V. Pound, *Phys. Rev.*, **74**, 679 (1948).
(35) C. P. Slichter and D. Ailion, *Phys. Rev. A*, **135**, 1099 (1964); D. Ailion, *Adv. Magn. Reson.*, **5**, 172 (1972).
(36) H. Kessemeier and R. E. Norberg, *Phys. Rev.*, **155**, 321 (1967).
(37) J. M. Deutch and I. Oppenheim, *Adv. Magn. Reson.*, **3**, 43 (1968).
(38) J. Schaefer, E. O. Stejskal, and R. Buchdahl, *Polym. Prepr., Am. Chem. Soc., Div. Polym. Chem.*, **17(2)**, 17 (1976).
(39) G. P. Jones, *Phys. Rev.*, **148**, 332 (1966).
(40) N. I. Lin and J. Jonas, *J. Magn. Reson.*, **18**, 444 (1975).
(41) M. V. Volkenstein, "Configurational Statistics of Polymeric Chains", Interscience, New York, N.Y., 1963.
(42) P. J. Flory, "Statistical Mechanics of Chain Molecules", Interscience, New York, N.Y., 1969, p 92; M. V. Volkenstein, ref 41, p 490.
(43) H. J. Hilhorst and J. M. Deutch, *J. Chem. Phys.*, **63**, 5153 (1975).
(44) H. E. Anderson, *J. Chem. Phys.*, **52**, 2821 (1970).
(45) Reference 9, p 12, refers to a correlation time describing microscopic motion as a "relaxation time τ". The confusion is in the choice of nomenclature only. We reserve the term "relaxation time" to describe phenomenonologically the NMR experiment.

(46) P. J. Flory, ref 42, p 35.
(47) G. Allen, D. C. W. Morley, and T. Williams, *J. Mater. Sci.*, **8**, 1449 (1973).
(48) G. A. Adam, A. Cross, and R. N. Haward, *J. Mater. Sci.*, **10**, 1582 (1975).
(49) R. J. Morgan and J. E. O'Neal, *J. Polym. Sci., Polym. Phys.*, **14**, 1053 (1976).
(50) A. E. Tonelli, *Macromolecules*, **4**, 653 (1971).
(51) P. Botherel and G. Fourche, *J. Chem. Soc., Faraday Trans. 2*, **69**, 441 (1973).
(52) P. J. Flory, *Macromol. Chem.*, **8**, 1 (1973); reprinted as *Rub. Chem. Technol.*, **48**, 513 (1975).
(53) R. F. Boyer, *J. Macromol. Sci., Phys.*, in press.
(54) E. W. Fischer, J. H. Wendorff, M. Dettenmaier, G. Lieser, and I. Voigt-Martin, *Polym. Prepr., Am. Chem. Soc., Div. Polym. Chem.*, **15**(2), 8 (1974).
(55) H. Benoit, *Polym. Prepr., Am. Chem. Soc., Div. Polym. Chem.*, **15**(2), 324 (1974).
(56) A. Pines, M. G. Gibby, and J. S. Waugh, *Chem. Phys. Lett.*, **15**, 373 (1972).
(57) J. Heijboer, "Physics of Non-crystalline Solids", North-Holland Publishing Co., Amsterdam, 1965.
(58) A. E. Tonelli, *Macromolecules*, **5**, 558 (1972). However, quite different results have been obtained by other calculations. See, for example, F. Laupretre and L. Monnerie, *Eur. Polym. J.*, **10**, 21 (1974).
(59) See, for example, ref 9, p 182.
(60) For recent reviews, see R. F. Boyer, *Polym. Eng. Sci.*, **8**(3), 161 (1968); J. A. Sauer, *J. Polym. Sci., Part C*, **32**, 69 (1971); R. F. Boyer, "Polymeric Materials", American Society of Metals, Metals Park, Ohio, 1975, p 277; P. I. Vincent, *Polymer*, **15**, 111 (1974).
(61) H. Heijboer, *Kolloid-Z.*, **171**, 7 (1960); L. E. Nielsen, "Mechanical Properties of Polymers", Van Nostrand-Reinhold, Princeton, N.J., 1962, p 209.
(62) Reference 9, p 127.
(63) Reference 9, p 125.
(64) Y. Ishida, *Kolloid-Z.*, **174**, 124 (1961).
(65) W. E. Wolstenholme, *J. Appl. Polym. Sci.*, **6**, 332 (1962).
(66) J. C. Radon and C. E. Turner, *Eng. Fract. Mech.*, **1**, 411 (1969).
(67) F. A. Johnson, A. P. Glover, and J. C. Radon, "Symposium on the Mechanical Behavior of Materials", Material Science, Japan, 1974, p 141.
(68) L. C. Cessna, *Polym. Prepr., Am. Chem. Soc., Div. Polym. Chem.*, **15**, 229 (1974).
(69) See, for example, E. H. Andrews, "Fracture in Polymers", Elsevier, New York, N.Y., 1968, p 71.
(70) A. Papoulis, "Probability, Random Variables, and Stochastic Processes", McGraw-Hill, New York, N.Y., 1965, p 338.
(71) A. Abragam, "Principles of Nuclear Magnetism", Oxford, 1961, p 271.
(72) Typical reservations are expressed by G. E. Roberts and E. F. T. White, "The Physics of Glassy Polymers", R. N. Haward, Ed., Applied Science, London, 1973, p 194; and I. M. Ward, "Mechanical Properties of Solid Polymers", Wiley, New York, N.Y., 1971, p 334.
(73) S. S. Sternstein, ref 16, p 369.
(74) A. S. Argon, ref 16, p 411.
(75) J. Schaefer, *Bull. Am. Phys. Soc.*, **21**, 443 (1976).
(76) D. Hull, ref 16, p 487.
(77) J. S. Waugh as cited in L. Müler, A. Kumar, and R. R. Ernst, *J. Chem. Phys.*, **63**, 5490 (1975); R. K. Hester, J. L. Ackerman, B. L. Neff, and J. S. Waugh, *Phys. Rev. Lett.*, **36**, 1081 (1976).

Molecular and Crystal Structures of Poly(ethylene oxybenzoate): α Form

Hiroshi Kusanagi, Hiroyuki Tadokoro,* Yozo Chatani, and Kazuaki Suehiro[1]

Department of Polymer Science, Faculty of Science, Osaka University, Toyonaka, Osaka 560, Japan. *Received August 11, 1976*

ABSTRACT: The crystal structure of poly(ethylene oxybenzoate) α form was determined by x-ray analysis and intra- and intermolecular interaction potential energy calculations, i.e., the crystal structure model was refined by using a packing energy minimization method prior to the least-squares refinement in x-ray analysis. The unit cell is orthorhombic, $P2_12_12_1$, with a = 10.49 Å, b = 4.75 Å, and c (fiber axis) = 15.60 Å. The two antiparallel (2/1) helical chains are located at the center and the corner of the unit cell. The internal rotation angles are

$$\text{——CH}_2\text{——(——O——Ph——CO——O——CH}_2\text{——CH}_2\text{——)——}$$
$$-186^\circ \qquad -13^\circ \ -15^\circ \ -172^\circ \ -102^\circ \ -59^\circ$$

where the angle (−13°) is for the virtual bond (O–Ph–C) and the dihedral angle (−15°) is defined by the planes of the benzene ring and the ester group. The chain has a zigzag conformation of large scale, one monomeric unit being a large zigzag unit. The low crystallite modulus of the α form is explained by this molecular structure.

Poly(ethylene oxybenzoate), $[-OPhCOOCH_2CH_2-]_n$, is an aromatic poly(ester ether), the chemical structure of which is similar to poly(ethylene terephthalate), $[-OCOPhCOOCH_2CH_2]_n$. The only difference is at the linkage adjacent to the aromatic ring (left side in the formula): ether or ester. This difference, however, leads to the remarkable difference of the molecular conformations and crystal structures, which should be reflected in the various physical properties. Poly(ethylene terephthalate) has an almost fully extended molecular conformation in the crystal[2] and the high crystallite modulus 108 × 10^{10} dyn/cm^2.[3] On the other hand, poly(ethylene oxybenzoate) has two crystal modifications, α and β forms.[4] The fiber period 15.60 Å of the α form suggests a fairly large contraction of the molecular chain, while that of the β form 18.9 Å corresponds to the almost fully extended conformation. The α form has a very low crystallite modulus 6 × 10^{10} dyn/cm^2,[5] which is lower by about one order than that of poly(ethylene terephthalate). In the present paper, we determined the molecular and crystal structures of the α form of poly(ethylene oxybenzoate) and discussed the structure–property relationship.

A monoclinic unit cell including a planar zigzag molecular model with the cis CH_2–CH_2 bond,[4] and orthorhombic unit cell with a = 10.46 Å, b = 4.76 Å, c (fiber axis) = 15.60 Å,[5] and the space group $P2_12_12_1$[6] was reported. The crystal structure of the α form, however, has not yet been analyzed successfully, because of difficulty in the setting up of molecular models as will be mentioned in the later sections. Hence we utilized the calculation of the intramolecular interaction energy for selecting suitable molecular models, considering the successful results of application of the energy calculation to the structure analyses: polyisobutylene,[7] poly(*tert*-butylethylene oxide),[8] poly(β-ethyl-β-propiolactone)[9] and so on. In the present study, besides the intramolecular interaction energy calculation, the refinement of the crystal structure model was made by the calculation of intermolecular interaction energy.

Experimental Section

Samples. Uniaxially oriented specimens of the α form for x-ray measurement were prepared by stretching filaments to about 3.5 times the original lengths at 80 °C followed by annealing at 200 °C for 5 h under tension using a metal holder. A doubly oriented specimen was